IEEE Access
Multidisciplinary | Rapid Review | Open Access Journal

Received February 5, 2021, accepted March 4, 2021, date of publication March 22, 2021, date of current version April 13, 2021.

Digital Object Identifier 10.1109/ACCESS.2021.3065246

A Novel Coarse-to-Fine Sea-Land Segmentation Technique Based on Superpixel Fuzzy C-Means Clustering and Modified Chan-Vese Model

EMAN ELKHATEEB[1], HASSAN SOLIMAN[1], AHMED ATWAN[2], MOHAMMED ELMOGY[1], (Senior Member, IEEE), KYUNG-SUP KWAK[3], (Life Senior Member, IEEE), AND NAGHAM MEKKY[1]

[1]Department of Information Technology, Faculty of Computers and Information Science, Mansoura University, Mansoura 35516, Egypt
[2]Faculty of Computer Sciences and Information Technology, Northern Border University, Arar 73222, Saudi Arabia
[3]Department of Information and Communication Engineering, Inha University, Incheon 22212, South Korea

Corresponding author: Kyung-Sup Kwak (kskwak@inha.ac.kr)

This work was supported by National Research Foundation of Korea-Grant funded by the Korean Government (Ministry of Science and ICT)-NRF-2020R1A2B5B02002478).

ABSTRACT The sea-land segmentation for optical remote sensing images (RSIs) has a valuable role in water resources and coastal zones management. However, it is challenging because optical RSIs mainly suffer from low contrast, intensity inhomogeneity with mixed pixels, and large image size with redundant information. This paper introduces a novel coarse-to-fine sea-land segmentation method that incorporates Superpixel Fuzzy C-Means (SPFCM) and a Modified Chan-Vese active contour model (MCV). First, the image is over-segmented into superpixels to reduce the information redundancy and utilize spectral and spatial information. The SPFCM employs local relationships among neighboring superpixels to cluster the superpixels based on their color and texture features, deal with mixed pixels, and produce coarse segmentation results. The CV depends on the initial contour. If the contour is incorrectly initialized, the CV may trap in local minima and needs many iterations. The purpose of the SPFCM result is to provide an automatic initial contour for an MCV model instead of manual initialization to improve the CV model's performance. Finally, color and texture features are combined in vector-valued images to solve the traditional CV's problems to deal with complicated nature images with intensity inhomogeneity or rich texture features to produce fine segmentation results. The proposed method is evaluated and achieved an average accuracy of 98.9%, an average Jaccard Similarity Coefficient (JSC) equals 97.1%, an average Disc Similarity Coefficient (DSC) equals 98.5%, and an average recall equals 99.3%. The proposed method results are promising, and it outperformed the results of other state-of-the-art sea-land segmentation methods.

INDEX TERMS Sea-land segmentation, superpixel fuzzy c-means, Chan-Vese model, remote sensing.

I. INTRODUCTION

In recent years, optical remote sensing images (RSIs) have a vital role in water resources monitoring, coastal zones, and maritime safety management. They can easily acquire detailed information on a large area about maritime and coastal zones. These zones are considered the main environmental socio-economic in most parts of the world. However, these zones are among the most vulnerable to dynamic natural processes, such as erosion, accretion, flooding, sediment transport, and climatic changes. These hazards influence these zones and decrease coastal land resources [1], [2].

The sea-land segmentation (SLS) for the optical RSIs is considered one of the most remote sensing applications, which is a key for decision-makers for national development and environmental protection. SLS results have an essential role in many various applications, such as ship detection, coastline extraction, oil leakage detection, control of maritime traffic, ocean surveillance, and maritime safety management [3]–[6]. Also, it has a role in detecting illegal smuggling, monitoring the changes in coastal zones, and water resources management [4], [7]–[9].

The associate editor coordinating the review of this manuscript and approving it for publication was Giovanni Pau.

The purpose of SLS is to separate RSI into sea and land regions based on the selected homogeneity measures (e.g., intensity, color, and texture). The segmentation result is a set of contours (boundaries) of objects or a set of segments that cover the entire image [4], [10], [11]. In the past decades, the manual SLS has been possible based on the research area's prior geographical information as a standard reference. It has faced many problems, like taking much time and need substantial efforts. It is also difficult to obtain accurate geographical information about some areas [12], [13]. Consequently, the implementation of automatic SLS approaches can provide precise results about the research cases and do not take much time compared to the manual segmentation.

The sea-land segmentation of the optical RSIs is considered a challenging problem because of many factors, such as a complicated texture of land cover area, intensity inhomogeneity, and low contrast between sea and land regions. Optical RSIs are affected by different degrees of Gaussian noise during image acquisition. The large image size with redundant information. Also, the presence of mixed pixels between sea and land regions, such as shadow, could be dark as a sea, and waves in the sea region could be classified as land [7]. All these challenges can impact the segmentation task [7]–[9], [15], [16].

Many segmentation algorithms have been developed for various applications. Among these segmentation algorithms, active contour models (ACMs) and fuzzy clustering methods have received more attention in the image segmentation field due to their good performance. ACMs have gained more and more attention in the image segmentation field. They can achieve better segmentation accuracy. Active contour models can deal with topological changes of contour curves [14]–[17].

Generally, ACMs can roughly fall into two categories: edge-based ACMs and region-based ACMs. In edge-based ACMs, the evolving curve can move toward the object boundaries based on the image gradient information. But these models are sensitive to the initial contour and cannot extract the objects with weak or noisy boundaries. On the other hand, region-based ACMs use image information, e.g., intensity, color, and texture, to guide the curve toward the object boundaries. These models can extract objects with weak and noisy boundaries. Also, they are less sensitive to initial contour than edge-based ACMs. Chan- Vese (CV) model is considered one of the region-based ACMs. It is the most widely used algorithm in image segmentation. The CV model utilizes the global intensity to guide the curve toward the object boundaries [16]–[19].

There are many clustering methods such as K-means, graph cut, and fuzzy C-Means (FCM) methods. K-means is a hard clustering method, which clusters each pixel just to one cluster. However, this constraint leads to some difficulties in RSI segmentation due to intensity overlapping between pixels within RSI, low contrast, and intensity inhomogeneity. The graph cut method produces a good result, but it has high computational complexity due to the large size of RSI and the redundant information. On the other hand, the FCM algorithm is one of the most widely used fuzzy clustering methods in image segmentation. The motivation behind the usage of FCM is that it clusters one pixel to more than one cluster by assigning a membership value to each pixel. It makes the FCM handle mixed pixels, deal with fuzzy and uncertain data in RSI and provide good performance. The traditional FCM clustering algorithm often failed to deal with the aforementioned challenges because FCM considers only spectral information and does not incorporate pixels' spatial information into its account. However, the improved FCM by incorporating local spatial information may produce high computational complexity because of the repetition of the distance computation between the centers of clusters and pixels within a local neighboring window. Besides, neighbors' regular window often breaks up the real, local spatial structure of images, which produces poor segmentation [20]–[24].

The motivation behind the Chan-Vese active contour model's usage is that the CV model is flexible, strong, and satisfactorily segments the objects with weak boundaries. It can automatically change its topology to achieve an optimum segmentation for image regions with smooth or discontinuous complex boundaries [9]. However, the traditional CV model can achieve poor results for images with intensity inhomogeneity and low contrast. Also, it is sensitive to manual initialization. If the contour is incorrectly initialized, the traditional CV model may trap local minima and needs many iterations.

This paper presents a novel unsupervised coarse-to-fine SLS technique for the natural colored RSIs to overcome the aforementioned limitations. It integrates Superpixel FCM (SPFCM) clustering and a modified CV active contour model. This paper has three main contributions:

- The image is over-segmented into superpixels to reduce the information redundancy. Besides, it utilizes spectral and spatial information to produce superpixels.
- The SPFCM clustering approach produces coarse sea-land segmentation results, which provides an automatic initial contour for the CV active contour model instead of manual initialization to improve the CV model's performance.
- Spectral color and texture features are combined in vector-valued images to improve the CV model and solve its limitations to those complicated nature images with intensity inhomogeneity or rich texture features and produce fine segmentation results.

The rest of the paper is arranged as follows. Section II presented the related work of the sea-land segmentation problems and discussed different methods and their related limitations. Section III explains the preliminaries of the basic methods which are utilized in the proposed segmentation technique. Section IV discusses the proposed segmentation technique in detail. Section V describes the used dataset, evaluation metrics, and experimental results and discussions. In the end, Section VI presents the conclusion and future work.

II. LITERATURE REVIEW

Many efforts have been made to develop various sea-land segmentation methods and coastline extraction from different geographical regions and satellite images. The recent studies of fuzzy c-means and active contour models are also reported with their advantages and limitations. For example, Aedla *et al.* [2] utilized a clipped histogram equalization to improve the image's contrast. After that, an adaptive threshold based on the mean and the standard deviation was used for the segmentation task. This method failed to deal with the complicated distribution of the intensity and the complex scene. This method depended on the intensity of pixels without any considerations of neighboring pixels.

Xia *et al.* [25] used a gray intensity feature of the image and the Local Binary Pattern (LBP) to define the texture feature. Then, a threshold value was applied to segment the image. However, this method required post-processing operations and was sensitive to the noise.

Zhuang *et al.* [26] utilized a gradient feature map (GFM) to form the sum area table (SAT) and reconstruct an integral image. An adaptive threshold based on the texture and the structure information was used for the segmentation task. In the end, the morphological operations were applied to close holes. However, the noise impacted GFM.

Dejan *et al.* [27] utilized a locally adaptive threshold to classify the enhanced image into sea and land regions. This method was fast and accurate. However, the weather conditions and the low contrast between water and land areas influenced an accurate coastline extraction.

You and Li [28] proposed an SLS method based on a sea region's statistical model (SMS). In the beginning, the sea area was extracted by the Otsu thresholding method. Then, SMS was applied to segment the image into sea and land regions. Finally, the difference in SMS variance between sea and land was used to remove the misclassified land regions. This method performed well, robust, and computationally efficient. However, there was a misclassification because of the complicated distribution of the land regions.

Ma *et al.* [13] introduced a hierarchical method by incorporating the modified Otsu segmentation method with intensity and texture features. Then, the modified Otsu method was applied to extract land boundaries. This method was computationally effective under different conditions.

Wang *et al.* [29] enhanced the structural and texture information by incorporating the gradient feature map and the pyramid integral image reconstruction on a different scale. Then, the adaptive threshold method was applied to obtain the sea and the land areas. This method was stable in day and night scenes.

Liu *et al.* [20] clustered the image into sub-regions based on the improved multiscale normalized cut segmentation by incorporating the gray intensity and local entropy features. The sub-regions were merged to produce the initial segmentation results to improve the CV model's final segmentation results. However, the convergence rate of the CV model was slow. This method was not computationally efficient.

Modava and Akbarizadeh [30] applied the Spatial Fuzzy Clustering (SFC) method, which combined spatial constraints for the initial segmentation phase. Then, the level set active contour method was applied to refine the segmentation results. This method reduced the manual contour initialization. However, the SFC method could not handle mixed pixels because of the image's complicated characteristics.

Wu *et al.* [14] proposed a fuzzy-based active contour model for image segmentation called Kernel Fuzzy Active Contour (KFAC). This method incorporated a fuzzy logic and kernel metric into an active contour model. The fuzziness function provided the model with a strong ability to reject local minima. Since the KFAC model depended on global image information, it has difficulties segmenting the image with intensity inhomogeneity or rich texture.

Fang *et al.* [15] proposed a new fuzzy region-based active contour model based on weighting global and local fitting energy to segment the images. The local spatial image information was incorporated into fuzzy region energy. The results proved the efficiency of this method. However, this model failed to segment images when the image object is very similar to the background region.

Fang *et al.* [19] incorporated new global and local fitting energy functions into fuzzy-based active contour models for balancing the weights of the object and background regions. This method provided good results for segmenting the images with intensity inhomogeneity. However, this method failed to deal with the rich texture image.

Othman [31] proposed a new segmentation method for satellite imagery based on the Chan-Vese model with a saliency map. Besides, bilateral filter and histogram equalization were utilized to preserve the edges and enhance the satellite image, respectively. As shown in the results, the CV model is sensitive to manual initialization and produced poor results. Also, saliency map estimation is based on human-eye modeling, which could not interpret all objects.

Rajinikanth *et al.* [32] developed a hybrid method to extract fetal head periphery. This method preprocessed the image using the Jaya algorithm and Otsu's method to enhance the head section. Then, the CV model and level set segmentation methods were utilized to extract the fetal head section. This method achieved good accuracy. However, the CV was sensitive to initial contour.

In summary, as discussed in previous related work studies, the discussed studies achieved unsatisfactory results due to some limitations, such as low contrast of RSIs, large image size with redundant information, and segmentation process based on threshold methods without incorporation spatial and texture information. They could also not deal with the data's fuzzy and uncertainty because RSIs have mixed pixels and data inhomogeneity. Also, the CV model is sensitive to manual initialization.

We present a novel coarse-to-fine sea-land segmentation technique for the natural colored RSIs to overcome the aforementioned limitations. It integrates superpixel FCM clustering (SPFCM) and CV active contour modeling. Firstly, to reduce the information redundancy, the image is oversegmented into superpixels based on spectral and spatial information of pixels in the image. Secondly, the SPFCM clustering approach employs the local relationship among neighboring superpixels to cluster superpixels based on the color and texture features to produce coarse sea-land segmentation results. The purpose of the SPFCM result is to provide the initial contour for the CV model instead of manual initialization to improve the CV model's performance. Finally, spectral color and texture features are combined in vector-valued images to improve the CV model to solve its limitations to those complicated nature images with intensity inhomogeneity or rich texture features and produce fine segmentation results.

III. BASIC CONCEPTS

This section explains the preliminaries of the basic methods which are utilized in the proposed method. These methods are divided into the preprocessing, feature extraction, and segmentation methods, which are discussed in the following subsections.

A. SUPERPIXEL COMPUTING

Generally, the superpixel algorithms group similar pixels into meaningful regions based on the image's local spatial information. They have many advantages, such as capturing image redundancy, reducing the subsequent processing tasks, and providing an appropriate form for image feature computing. There are many algorithms to produce superpixels, such as the graph-based and gradient-based methods. Achanta *et al.* [33] presented a comparative study of the superpixel computing methods. The simple linear iterative clustering (SLIC) method is used to produce the superpixels. It has many advantages, including easy to use, faster, more memory efficient, and adheres to the image's boundary. Besides, it improves segmentation performance as compared with other methods. In SLIC, the color and the spatial information have been used to cluster the pixels in CIE LAB color space locally. Every pixel label is iteratively updated via the searching process of the nearest cluster center of the pixel in a local space, which is closely related to the size of the superpixels [33]. The similarity measurement in SLIC is expressed by Eq. (1-3) [34]:

$$d\,(i, C) = d_{lab} + \frac{m}{SP} d_{xy} \tag{1}$$

$$d_{lab} = \sqrt{(l_c - l_i)^2 + (a_c - a_i)^2 + (b_c - b_i)^2} \tag{2}$$

$$d_{xy} = \sqrt{(x_c - x_i)^2 + (y_c - y_i)^2} \tag{3}$$

where d_{lab} refers to the difference in the color between two pixels. d_{xy} refers to the spatial distance between two pixels. (x, y) refers to the spatial location of the pixel. $d\,(i, C)$ measures the proximity between the i^{th} pixel and the C^{th} cluster center. The weight parameter (m) balances between color and spatial information in the proximity measure. The size of the desired superpixel is $SP \times SP$, where $SP = \sqrt{N/C}$, N refers to the number of image pixels, and C refers to the number of superpixels.

B. TEXTURE EXTRACTION METHODS

Texture can be considered a good feature to identify textural objects since it represents the variability of local intensity and patterns inside the surface of objects [35]. Texture analysis is considered an important feature in various problems, such as segmentation and classification of medical imaging and remote sensing. Statistical, structural, model-based, and signal processing-based are considered the four main categories for texture analysis methods used to extract the image's texture features. In this paper, we combined local entropy and Gabor texture features.

Statistical methods are considered the most popular texture analysis methods, which can be used for all types of textures due to their simplicity. They can also be incorporated with some other methods to improve the efficiency of the image segmentation method. The local entropy method that belongs to the statistical analysis method is an attribute that measures the randomness of the gray-level distribution of the image. Entropy extracts the dissimilarity of each local patch [36]. Given a center pixel (x, y) in a local patch of the input image, the local entropy is calculated by Eq. (4) [20], [37].

$$T_{(x,y)\cdot R} = -\sum_{i=0}^{255} \tilde{p}_i \log(\tilde{p}_i) \tag{4}$$

where i denotes the gray level. $\tilde{p}_i$ indicates the ratio of the pixels whose gray value is i within the local patch. R denotes the size of the local patch, which is set to 9.

The two-dimensional (2D) Gabor filter with different scales and orientations is utilized to capture the texture information. It has been widely used in the field of image processing because it is an effective texture extraction method. In this paper, the Gabor filter is utilized to extract the texture from the input image. The general form of the real part is defined by Eq. (5) [38].

$$g\,(x, y; \lambda, \theta, \sigma) = \exp\left(-\frac{x'^2 + y'^2}{2\sigma^2}\right) \exp\left(i\left(2\pi \frac{x'}{\lambda}\right)\right) \tag{5}$$

$$x' = x\,cos\theta + y\,sin\theta \tag{6}$$

$$y' = -x\,sin\theta + y\,cos\theta \tag{7}$$

where λ refers to the wavelength of the sinusoidal function, and θ refers to the orientation. σ denotes the standard deviation of the Gaussian envelope. Here, $\lambda = \{2, 5, 8\}$, $\theta = \{0, 45, 90, 135\}$, and $\sigma = \{1, 2, 3, 4\}$.

C. FUZZY C-MEANS CLUSTERING

FCM is one of the effective fuzzy clustering algorithms [39], [40]. The image segmentation problem can be considered a

clustering problem. FCM is widely utilized for the image segmentation task because it efficiently deals with uncertainty and ambiguity compared to hard clustering. Given a set of data points $X = \{x_1, x_2, \ldots, x_S\}$ and the cluster centers $v = \{v_1, v_2, \ldots, v_{\bar{C}}\}$ [41]. Each data point can be assigned to different clusters at the same time with some weight called a membership, which indicates how much the data point belongs to a particular cluster [42]–[45].

D. CHAN- VESE MODEL

Chan-Vese (CV) model [46] is one of the widely used techniques in image segmentation. The CV model is one of the region-based ACMs. It segments the image into two regions (e.g., object and background). In the CV model, image segmentation is considered an energy minimization problem. The CV model's principal idea is to find an optimal contour that partitions a given image into two regions, one representing the objects to be detected and the other representing the background.

In the image domain, an energy function expresses the curve or an initial contour. Under some constraints, the curve moves to the boundaries of the object via computing the difference between the intensity values of pixels inside the object and the background regions. The evolution of the CV curve depends on the region's homogeneity rather than the gradient magnitude of the image; therefore, it well segments the image, although there are weak boundaries [47], [48].

For a given image $I(x)$ on the image domain Ω, the following energy function of the CV model for scaler- valued image is minimized [49], [50]:

$$\begin{aligned} F(c_1, c_2, C_u) = {} & \mu.Length(C_u) + v.Area(inside(C_u)) \\ & + \lambda_1 . \int_{inside(C_u)} |u_0(x,y) - c_1|^2 dxdy \\ & + \lambda_2 . \int_{outside(C_u)} |u_0(x,y) - c_2|^2 dxdy \end{aligned} \quad (8)$$

where C_u represents the curve. The constants c_1 and c_2 are the average intensities inside and outside the curve, respectively. A regularizing term, such as the length of C_u and the area inside C_u to control the smoothness of the boundary. μ refers to the length term that is considered a regularizing term. Also, it has a scaling role. For large μ, objects of larger sizes are only detected. Also, only objects of smaller sizes are detected If μ is small. The coefficients λ_1 and λ_2 are fixed parameters [49], [50].

Using the level set function to represent the curve, that is, the curve is the zero-level set function $\phi(x, y)$, we can replace the unknown variable C_u by $\phi(x, y)$ function, such that [50]:

$$\begin{cases} C_u = \{(x,y) \,|\phi(x,y) = 0\} \\ inside(C_u) = \{(x,y) \,|\phi(x,y) > 0\} \\ outside(C_u) = \{(x,y) \,|\phi(x,y) < 0\} \end{cases} \quad (9)$$

By applying the gradient descent method in the variational level set function $\phi(x, y)$, the energy function can be written as in Eq. (10) [49]–[51]:

$$\begin{aligned} & F(c_1, c_2, \phi) \\ & = \mu \int_\Omega \delta(\phi(x,y)) \,|\nabla\phi(x,y)| \, dxdy \\ & \quad + v \int_\Omega H(\phi(x,y)) \, dxdy \\ & \quad + \lambda_1 \int_\Omega |u_0(x,y) - c_1|^2 H(\phi(x,y)) \, dxdy \\ & \quad + \lambda_2 \int_\Omega |u_0(x,y) - c_2|^2 (1 - H(\phi(x,y))) \, dxdy \end{aligned} \quad (10)$$

while the Heaviside step function can be expressed as [49]–[51]:

$$H(\phi(x,y)) = \begin{cases} 1, & if\ \phi(x,y) > 0 \\ 0, & else \end{cases} \quad (11)$$

Heaviside step function can be slightly smoothed. Its derivative is then a smoothed delta function [50], [51]:

$$\delta(\phi) = \frac{d}{d\phi} H(\phi) \quad (12)$$

$F(c_1, c_2, \phi)$ with respect to ϕ and parameterizing the descent direction by an artificial time t, the equation in $\phi(x, y, t)$ is defined as in Eq. (13) [52]:

$$\begin{cases} \dfrac{\partial\phi}{\partial t} = \delta(\phi) \left[\mu.div\left(\dfrac{\nabla\phi}{|\nabla\phi|}\right) - v - \lambda_1 (u_0 - c_1)^2 \right. \\ \qquad \left. + \lambda_2 (u_0 - c_2)^2\right] \\ \phi(x, y, 0) = \phi_0(x, y) \end{cases} \quad (13)$$

IV. THE PROPOSED TECHNIQUE

In this section, we discuss our proposed SLS method, which is called SPFCM-MCV. SPFCM-MCV stands for Superpixel Fuzzy C-Means and Modified Chan Vese model. Fig. 1 shows the proposed SPFCM-MCV technique framework. It is divided into three main phases, which are preprocessing, feature extraction, and segmentation phases. The first phase is the preprocessing phase, which includes two steps. First, the input image is transformed from RGB to HSV color space. It defines color in terms of hue (H), saturation (S), and brightness (V). Second, the image is over-segmented into superpixels using the SLIC method to reduce the information redundancy. The second phase is feature extraction. Multi-features include the spectral and texture extracted to encode each superpixel and characterize the sea and the land regions. The third phase is the segmentation phase, which includes two steps. The first one is to produce coarse segmentation results by applying the SPFCM method. The CV model's initial contour is then defined based on the SPFCM result, which reduces the number of iteration and computational time of the CV model. In the last one, the CV model is modified by incorporation the color and texture features to produce fine segmentation results. The phases are discussed in detail in the following subsections.

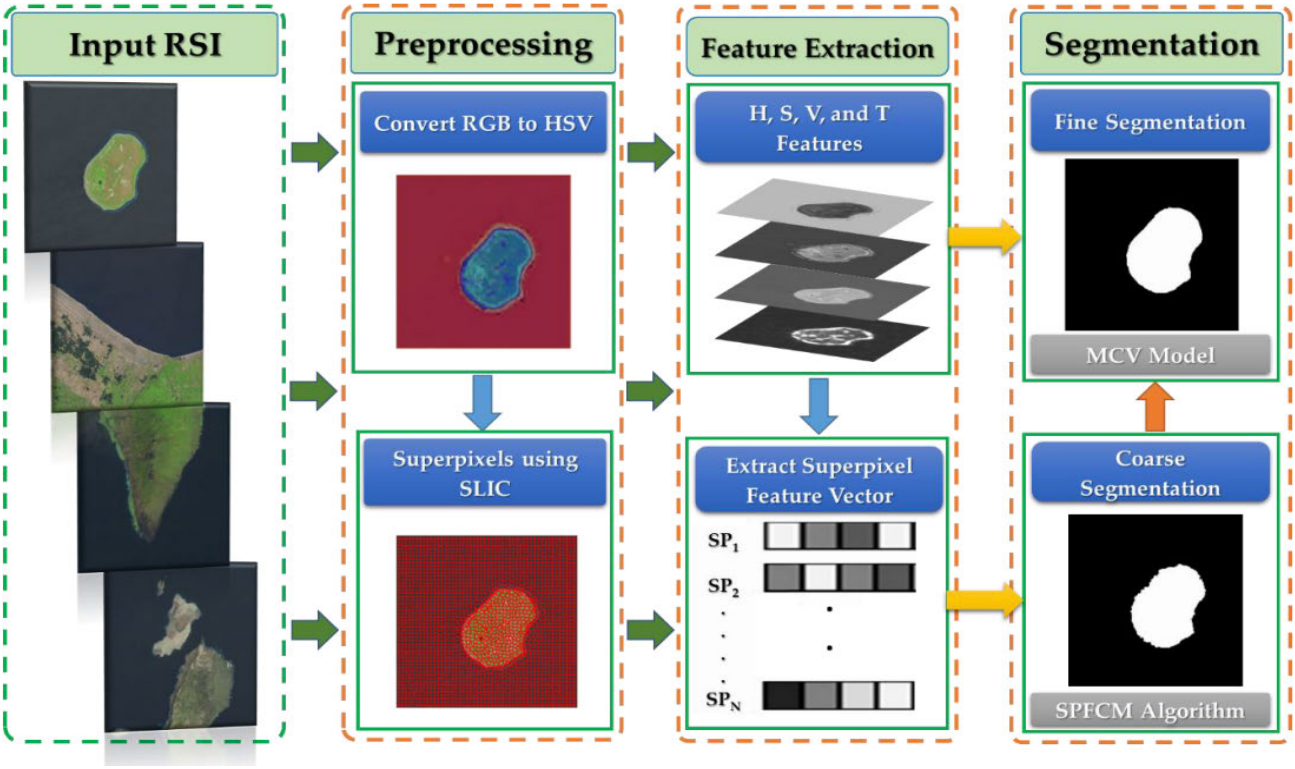

FIGURE 1. The framework of the proposed SPFCM-MCV Method.

A. THE PREPROCESSING PHASE

Many factors have adverse effects on segmentation results, such as noise, low contrast, illumination, weather conditions, and the large size of the images. Therefore, image preprocessing is considered an essential phase for the proposed method before feature extraction and image segmentation steps. This phase consists of two main steps. In the first step, the image is transformed from RGB to HSV color space. RGB is not suitable for this task as it is affected by illumination changes and low contrast. HSV is highly recommended to use in this task [53], [54]. HSV is invariant to changes in illumination and brightness. Chrominance (HS) is the spectral feature, and value (V) represents the brightness of the image. Superpixel computing is the second step of the image preprocessing phase. The traditional segmentation methods neglect the local similarity between pixels because they have performed on the pixel level. Besides, the sea-land image has a large size, and neighboring pixels are often similar in spectral and texture features, which lead to information redundancy, especially for the sea areas [7]. Therefore, the input image is over-segmented into superpixels, which can reduce the information redundancy in the image, minimizing the difficulty of successive processing tasks [44]. In this paper, the SLIC method is applied to compute superpixels due to its advantages, as previously explained.

The weight parameter m of SLIC balances color and spatial information in the proximity measure. When m is small, the produced superpixels have a higher boundary adherence but shape and size regularity decrease. Fig. 2 shows the results of SLIC superpixels corresponding to different values of m. As shown, for a larger value of m, the resulting superpixels have regular-shapes and do not fit well to the weak edges. Furthermore, a smaller value of m makes the SLIC more sensitive to the changes, and the superpixel boundaries do not appropriately fit to the image edges [55]. Therefore, m is set to 15 in this paper.

To evaluate the adherence ability of SLIC, the dataset is used to compute the average Boundary Recall (BR) that is defined by Eq. (14).

$$Boundary\ Recall = \frac{N1}{Ng} \tag{14}$$

where Ng refers to the count of the boundary pixels that are presented in the ground truth. $N1$ refers to the number of the boundary pixels in the ground truth (GT) for which there is a boundary pixel that falls within two pixels of the superpixel boundary. Fig. 3 shows the relationship between the size of superpixels and BR. The BR decreases with the increase of superpixel size. Also, m value impacts the adherence boundaries of superpixels [7]. Besides, superpixel size equals 80 and 100, which can achieve accurate results. Here, the superpixel size is set to 100 to reduce the processing time.

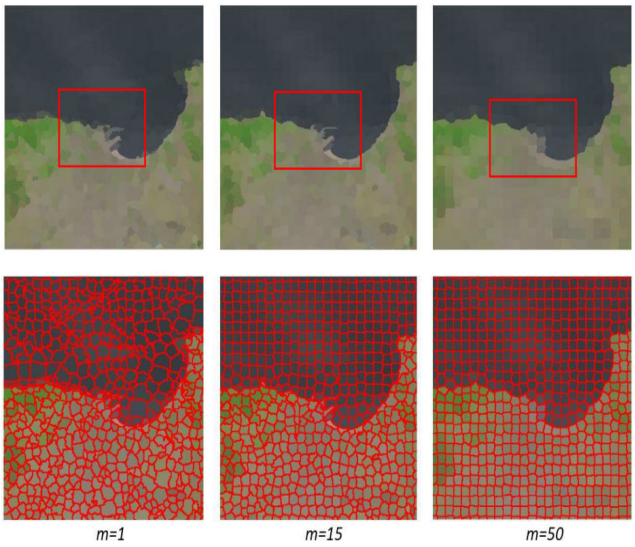

FIGURE 2. The results of the SLIC superpixels with different values of m.

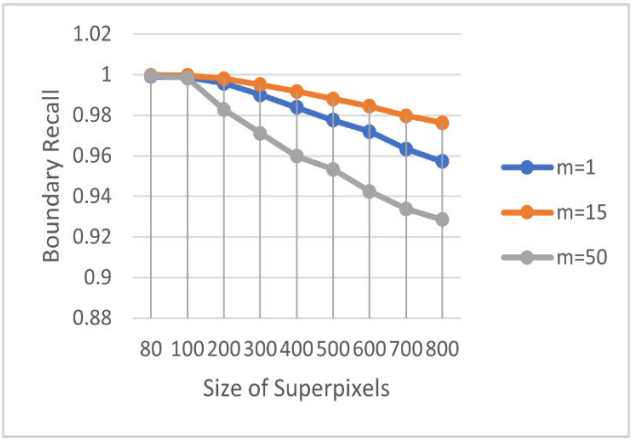

FIGURE 3. The BR of the SLIC method.

B. FEATURE EXTRACTION PHASE

During the observation of sea-land images, most sea areas have presented regular textures despite waves. The land area has been complicated distributions due to various objects on the earth [7], [56]. In this paper, the color and texture features have been utilized for encoding superpixels and distinguishing the sea and land areas [57]. Here, H and S are used as color features, and V is used as an intensity feature. Texture can be used to characterize the spatial arrangement of the intensities of the pixels in a region of a digital image [58].

In the remote sensing field, spectral information is not enough to segmentation spectrally heterogeneous landscape regions. The texture feature offers exciting possibilities to characterize different classes' structural heterogeneity, especially in sea and land regions [59]. There are many methods of texture extraction [26], [60], [61]. In this paper, local entropy and Gabor texture features are utilized as the texture feature descriptor due to their computational efficiency and stability. Here, texture features are extracted from the V channel. The feature vector of a pixel i is defined as $zi = [h_i^T, s_i^T, v_i^T, T_i^T]$, where $h_i^T, s_i^T, v_i^T, and\ T_i^T$ are the color (h_i^T, s_i^T), intensity, and texture vector of i, respectively. Every superpixel is encoded by computing the mean of zi of pixels within it. After the feature extraction process, the selected features have been normalized between 0 and 1 to clear the negative effect of different feature scopes.

C. THE SEGMENTATION PHASE

In this phase, the RSI is segmented according to the extracted features. So, this phase consists of coarse and fine segmentation steps. First, RSIs have some limitations, including redundant information, complicated distribution of the land area, and affected by noise. Also, the traditional methods have drawbacks, such as ignoring spatial information. They do not get immune to noise because they perform pixel-by-pixel segmentation, as previously explained. Therefore, SPFCM can capture the spatial information of superpixels. It incorporates the immediate neighborhood of each superpixel into the membership function. SPFCM also incorporates the spectral and texture features of superpixels for image segmentation. This step produces a coarse segmentation result in the next step as the CV model's initial contour.

MCV model is the second step of the segmentation phase and is used to fine-tune the results. As known, the traditional CV model can accurately extract the contour of the object. The SLS can be considered as an extraction of the contour between the sea and the land. The CV model segments these images with homogeneous intensity effectively. However, the CV model produces unsatisfactory results for naturally complicated images with intensity inhomogeneity, complex texture, and low contrast [51]. Therefore, spectral color and texture features are incorporated as discriminants of the MCV. The CV has a sensitivity to the initial contour. If the initial contour is incorrectly selected, the CV will take much time and produce inaccurate results [62]. So, the SPFCM coarse segmentation result provides the initial contour for the MCV model and reduces the computational time and number of iterations.

1) SUPERPIXEL FUZZY C-MEANS CLUSTERING

The main drawbacks of FCM are sensitivity to the imaging artifacts and the noise because FCM clusters the pixel without integrating any spatial information. Local spatial information can also be incorporated into FCM, which often produces a high computational complexity because of the repetition of the distance computation between the centers of clusters and pixels within a local neighboring window. Besides, neighbors' regular window often breaks up the real, local spatial structure of images, which produces poor segmentation results [22]. SPFCM was first proposed in [44] for medical image segmentation and achieved high accuracy in noisy images to solve these problems. Instead of utilizing pixels, SPFCM has used superpixels as clustering

objects. This algorithm has two advantages. The first one incorporates the immediate neighborhood of each superpixel into the membership function. It captures the superpixels' spatial information, which acts as a regularizer. It biases the solution toward piecewise-homogeneous labeling. Such regularization helps segment images corrupted by noise [63]. The last one takes statistical information of the superpixels into account to improve efficiency. The objective function is defined by Eq. (15) [44].

$$Jfcm = \sum_{i=1}^{\bar{C}} \sum_{j=1}^{Q} \gamma_j u_{ij}^{\bar{m}} \| \xi_j - v_i \|^2 + \frac{\alpha}{N_R} \sum_{i=1}^{\bar{C}} \sum_{j=1}^{Q} u_{ij}^{\bar{m}} \left(\sum_{\bar{s}_r \in \bar{N}_{\mathbf{j}}} \gamma_r \| \xi_r - v_i \|^2 \right) \quad (15)$$

where Q is the predefined number of the superpixels in the image, γ_j refers to the number of pixels in each superpixel $\bar{s}$j, and ξ_j denotes the feature vector of superpixel $\bar{s}$j. u_{ij} indicates the membership of superpixel $\bar{s}$j to the ith cluster. $\bar{N}_j$ indicates the set of adjacent superpixels that are neighboring to $\bar{s}$j, and N_R denotes to the cardinality of $\bar{N}_j$. $\|.\|$ indicates a norm metric that measures the Euclidean distance between cluster centroids and superpixels. The parameter $\bar{m}$ controls the fuzziness of the clustering results. The parameter α is used to control the effect of the neighborhood of superpixel. The membership function and the new cluster centers are expressed by Eq. (16), Eq. (17), respectively [44].

$$u_{ij} = \frac{1}{\sum_{k=1}^{\bar{C}} \left(\frac{\gamma_j \|\xi_j - v_i\|^2 + \frac{\alpha}{N_R} \sum_{\bar{s}_r \in \bar{N}_{\mathbf{j}}} \gamma_r \|\xi_r - v_i\|^2}{\gamma_j \|\xi_j - v_k\|^2 + \frac{\alpha}{N_R} \sum_{\bar{s}_r \in \bar{N}_{\mathbf{j}}} \gamma_r \|\xi_r - v_k\|^2} \right)^{\frac{1}{\bar{m}-1}}} \quad (16)$$

and

$$v_i = \frac{\left(\sum_{j=1}^{Q} u_{ij}^{\bar{m}} \left(\gamma_j \xi_j + \frac{\alpha}{N_R} \sum_{\bar{s}_r \in \bar{N}_{\mathbf{j}}} \gamma_r \xi_r \right) \right)}{\left(\sum_{j=1}^{Q} u_{ij}^{\bar{m}} \left(\gamma_j + \frac{\alpha}{N_R} \sum_{\bar{s}_r \in \bar{N}_{\mathbf{j}}} \gamma_r \right) \right)} \quad (17)$$

This membership value u_{ij} must satisfy the following constraints [45]:

$$0 \le u_{ij} \le 1, \quad for\ 1 \le i \le \bar{C}, 1 \le j \le Q,$$
$$0 < \sum_{j=1}^{Q} u_{ij} < Q, \quad for\ 1 \le i \le \bar{C}$$

SPFCM is applied to perform coarse segmentation to produce the initial contour for the MCV model, which reduces the number of iterations and computational time. In this paper, SPFCM clusters sea-land RSI into two clusters based on every superpixel's color and texture features, as listed in Algorithm 1 [44].

Z is the set of feature vectors of superpixels. $\bar{N}_j$ defines a set of neighbors of superpixels. $\bar{C}$ is the number of clusters. $\bar{m}$ controls the fuzziness of the cluster. α controls the effect of the neighborhood. ε is a predefined threshold. V indicates a vector of cluster centroids. The max-iters is the maxed iterations number. In this study, the value of $\bar{C}$, $\bar{m}$, α, ε, and max-iters is set to 2, 2, 0.2, 10^{-5}, and 100, respectively.

Algorithm 1 The Superpixel Fuzzy C-Means (SPFCM)

Input: $Z = \{\xi_1, \xi_2, \ldots, \xi_Q\}$, $\bar{N}_j$, $\bar{C}$, $\bar{m}$, α, ε, and *max-iters*
Output: u_{ij} and v_i

1. Initialize the centers of clusters randomly v_i, $i = 1, \ldots, \bar{C}$
2. **for** r $\mathcal{D}$ **0, 1, . . . , *to max_iters* do**
3. Calculate the membership u_{ij} by Eq. (16)
4. Update cluster centroids v_i by Eq. (17)
5. **if** $\left\| V_{(r\mathcal{C}1)} - V_{(r)} \right\| \le \varepsilon$ **then**
6. break
7. **End if**
8. **End for**

2) MODIFIED CHAN- VESE MODEL

The standard CV model has some limitations, such as it has unsatisfactory results in naturally complicated images with intensity inhomogeneity, complex texture, and low contrast. It depends on the intensity value of the pixel. Also, it has a sensitivity to the initial contour. The CV model has a relatively slow convergence rate [51]. Due to the large size of the sea-land RSIs, the iteration number is relatively large of the CV model. To solve these problems, color and texture features are used in the MCV model. The SPFCM coarse segmentation result produces the initial contour for the CV model instead of manual initialization, which reduces the number of iterations and computational time.

Chan and Vese [64] extended the traditional CV algorithm to detect objects in vector-valued images, such as color images. This study uses the CV model with different features, such as spectral and texture features. Let $u_{0,i}$ be the *ith* channel of an image on Ω, with $i = 1, 2, \ldots, N$ channels, and C_u the evolving curve. Each channel would contain the same image with some differences, for instance, color and texture feature image [49], [50]. The extension of the traditional CV model to the vector case is formulated by Eq. (18) [60].

$$\begin{aligned} F\left(\bar{c^+}, \bar{c^-}, C_u\right) &= \mu . Length\left(C_u\right) \\ &+ \int_{inside(C_u)} \frac{1}{N} \sum_{i=1}^{N} \lambda_i^+ \left| u_{0,i}(x,y) - c_i^+ \right|^2 dxdy \\ &+ \int_{outside(C_u)} \frac{1}{N} \sum_{i=1}^{N} \lambda_i^- \left| u_{0,i}(x,y) - c_i^- \right|^2 dxdy \end{aligned} \quad (18)$$

where μ refers to the length term that is set to 0.1. λ_i^+ and λ_i^- are positive parameters for each channel and set to 1. c_i^+ and c_i^- are the mean values of $u_{o,i}$ inside C_u and outside C_u, respectively.

The energy function can be written in a level set form as Eq. (19)

$$\begin{aligned} &F\left(\bar{c^+}, \bar{c^-}, \phi\right) \\ &= \mu . \int_\Omega \delta\left(\phi\left(x, y\right)\right) \left|\nabla \phi\left(x, y\right)\right| dxdy \\ &\quad + \int_\Omega \frac{1}{N} \sum_{i=1}^{N} \lambda_i^+ \left|u_{0,i}\left(x, y\right) - c_i^+\right|^2 H\left(\phi\left(x, y\right)\right) dxdy \\ &\quad + \int_\Omega \frac{1}{N} \sum_{i=1}^{N} \lambda_i^- \left|u_{0,i}\left(x, y\right) - c_i^-\right|^2 \\ &\quad \left(1 - H\left(\phi\left(x, y\right)\right)\right) dxdy \end{aligned} \tag{19}$$

Minimizing the energy with respect to the constants c_i^+, c_i^-, for $i = 1, \ldots, N$, we obtain:

$$c_i^+ = \frac{\int_\Omega u_{0,i}(x,y) H(\phi(x,y)) dxdy}{\int_\Omega H(\phi(x,y)) dxdy} \tag{20}$$

$$c_i^- = \frac{\int_\Omega u_{0,i}(x,y) (1 - H(\phi(x,y))) dxdy}{\int_\Omega H(\phi(x,y)) dxdy} \tag{21}$$

The regularized Heaviside function H_ϵ can be defined as:

$$H_\epsilon\left(\phi\right) = \frac{1}{2}\left(1 + \frac{2}{\pi} tan^{-1}\left(\frac{\phi}{\epsilon}\right)\right) \tag{22}$$

$$\delta_\epsilon\left(\phi\right) = H' = \frac{1}{\pi}\left(\frac{\epsilon}{\epsilon^2 + \phi^2}\right) \tag{23}$$

$F\left(\overline{c^+}, \overline{c^-}, \phi\right)$ with respect to ϕ and parameterizing the descent direction by an artificial time t, the following Euler Lagrange equation for $\phi\left(x, y, t\right)$ in Ω is defined as:

$$\begin{cases} \frac{\partial \phi}{\partial t} = \delta_\epsilon\left(\phi\right)\left[\mu . div\left(\frac{\nabla \phi}{|\nabla \phi|}\right) - \frac{1}{N}\sum_{i=1}^{N} \lambda_i^+ \left(u_{0,i} - c_i^+\right)^2 \right. \\ \qquad \left. + \frac{1}{N}\sum_{i=1}^{N} \lambda_i^- \left(u_{0,i} - c_i^-\right)^2\right] \\ \phi\left(x, y, 0\right) = \phi_0\left(x, y\right) \end{cases} \tag{24}$$

and with boundary condition on $\partial\Omega$ defined as:

$$\frac{\delta_\epsilon\left(\phi\right)}{|\nabla \phi|} \frac{\partial \phi}{\partial \vec{n}} = 0 \tag{25}$$

where $\partial \vec{n}$ indicates the unit normal at the boundary of Ω. Algorithm 2 shows the steps of the proposed SLS method based on color and texture features. Fig. 4 displays the results of the proposed method's segmentation phase. Also, it shows the curve evolution over time. As shown in the figure, the curve evolves well to the boundary of the object. The proposed model segments the image with mixed pixels and intensity inhomogeneity. The results and discussion are discussed in the results section.

V. RESULTS

This section describes the dataset, which is used in the proposed method and the experimental environment. Also, the segmentation performance measures are defined to evaluate the proposed method and compare it with other methods.

Algorithm 2 The Proposed SPFCM-MCV

Input: Natural colored (RGB) remote sensing image.
Output: The Segmented Image.
Step 1.
A. Convert RGB to HSV
B. Superpixel Computing by SLIC by Eq. (1)- Eq. (3)
Step 2.
C. Extract color feature (H, S), intensity (V), and texture feature using local Entropy and Gabor filter by Eq. (4), Eq. (5), respectively.
Step 3.
D. The coarse segmentation use SPFCM as in Algorithm 1.
E. Extract initial contour from the SPFCM result.
F. The fine segmentation using the MCV model by Eq. (24)

A. DATASET DESCRIPTION

In this paper, the natural-colored images have medium resolution and spatial resolution ≈30m from Landsat-7 ETM+ and Landsat-8 satellites. These images are used to evaluate the effectiveness of the presented method. They have been obtained from the USGS Global Visualization Viewer [65]. One hundred large images of different geographical locations have been obtained. They have been further cropped with [512 × 512] for the image. Two hundred images have been selected to form the sea-land dataset. The dataset images have complex characteristics of intensity and texture. Some images in the land regions are dark as the sea because of low contrast, and images with intensity inhomogeneity as shown in Fig. 5. This dataset's corresponding Ground-Truth has been labeled as in [4], [7] to estimate the presented technique's accuracy compared to other segmentation methods.

In this paper, the experiments have been performed on a PC with an Intel i5-2450M 2.5-GHz processor, 8-GB internal storage, the operating system is window 10, and the software platform is MATLAB R2020a.

B. MEASURING THE SEGMENTATION PERFORMANCE

The performance of the proposed technique and the comparative techniques is measured by using various performance measures, such as:

- Jaccard Similarity Coefficient (JSC) is also known as the intersection over union (IoU). It measures the similarity between the predicted image BW1 and the reference image BW2. It is defined as the cardinality of the intersection between two images divided by their union's cardinality. JSC is calculated by Eq. (26) [66].

$$JSC = \frac{|BW1 \cap BW2|}{|BW1 \cup BW2|} \tag{26}$$

- Dice Similarity Coefficient (DSC): It is widely used to measure the performance of segmentation methods. It measures spatial overlap between the predicted image BW1 and the reference image BW2. DSC values range from 0 to 1. If the DSC value is one, this means the greatest overlap between two images and vice versa.

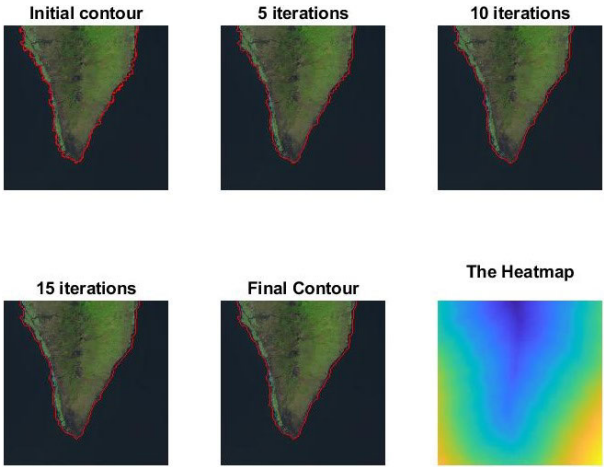

FIGURE 4. The curve evolution over the time. $\mu = 0.1$, iterations $= 40$.

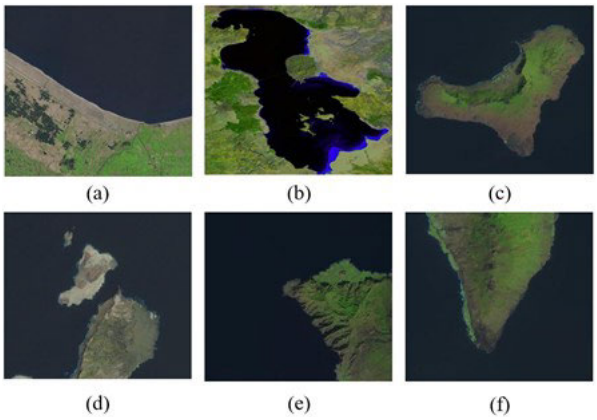

FIGURE 5. Examples of sea-land images.

DSC is defined by Eq. (27) [66].

$$DSC = \frac{2\,|BW1 \cap BW2|}{|BW1 \cap BW2|} \tag{27}$$

- Accuracy: It is the ratio of summations of correctly classified pixels and total pixels of the clustered image. It is defined by Eq. (28) [66].

$$Acc = \frac{(TP + TN)}{(TP + TN + FP + FN)} \tag{28}$$

- Recall or sensitivity: It refers to the proportion of total relevant results correctly classified by the proposed method. It is defined by Eq. (29) [67].

$$Recall = \frac{TP}{TP + FN} = \frac{Truepositive}{Totalactualpositive} \tag{29}$$

- Precision: It is the proportion of the relevant results to the total number of the relevant and irrelevant and results retrieved. It is defined by Eq. (30) [67].

$$\text{Precision} = \frac{TP}{TP + FP} = \frac{True\ positive}{Total\ predictive\ positive} \tag{30}$$

where TP is a true positive, and FP is a false positive. They refer to the correctly and incorrectly classified pixels as land pixels by the proposed technique. TN is a true negative, and FN is a false negative. They refer to the correctly and incorrectly classified pixels as sea pixels.

C. COMPARISON AND DISCUSSION

In this section, many comparisons and discussions have been performed and explained to prove the proposed technique's efficiency. First, the results of the traditional CV model with different manual initial contours are discussed. Then, FCM [39] and Spatial Fuzzy C-Means clustering (SFCM) [68] clustering methods have been compared with the proposed SPFCM technique. After that, there are many fuzzy-based ACMs that have been tested and compared with the proposed technique [14], [15], [19]. Finally, the performance of the proposed method is evaluated and compared with the state-of-the-art SLS techniques. LBP [25], SMS [28], SFC [30], and traditional CV model [46] segmentation methods are used for comparison with the proposed technique. On the other hand, the trade-off between spatial and texture information is investigated. Moreover, the proposed technique is tested on other applications area such as a skin lesion segmentation as in [69] and tested on natural images as in [70], [71].

1) RESULTS OF THE TRADITIONAL CV MODEL WITH DIFFERENT INITIAL CONTOURS

The CV model is tested with various types of initial contours for the segmentation task. The test results of the CV algorithm are shown in Fig. 6. The initial contours were displayed in white color in the first column, whereas the obtained final contours from the CV evolution displayed in red color in the second column. Also, the last column shows the segmented images that are corresponding to the initial contours. From Fig. 6, it is noticed that the only result that is corresponding to the initial contour in the first row achieves a successful segmentation result, to some extent, and the last two initial contours could not segment the image well. The CV algorithm can only segment the image that has homogenous regions. However, it has a bad segmentation result of the images that have an intensity inhomogeneity, and it has a sensitivity to the initial contours. CV algorithm lacks convexity, so it is possible to trap in a local minimum. As shown in the last two rows of Fig. 6, the initial contour is far away from the boundaries of all objects in the image. This is because the contours have been trapped firstly in local minimum before it covered all boundaries of all objects and reached global minima of the energy minimization function. So, this drawback achieved poor results.

2) COMPARISON OF SPFCM WITH CLUSTERING METHODS

FCM clustering method segments the image without incorporating any spatial information. So, it is sensitive to image inhomogeneity and artifacts. Fig. 7 proves the poor results of this drawback. As shown in the figure, there are misclassified

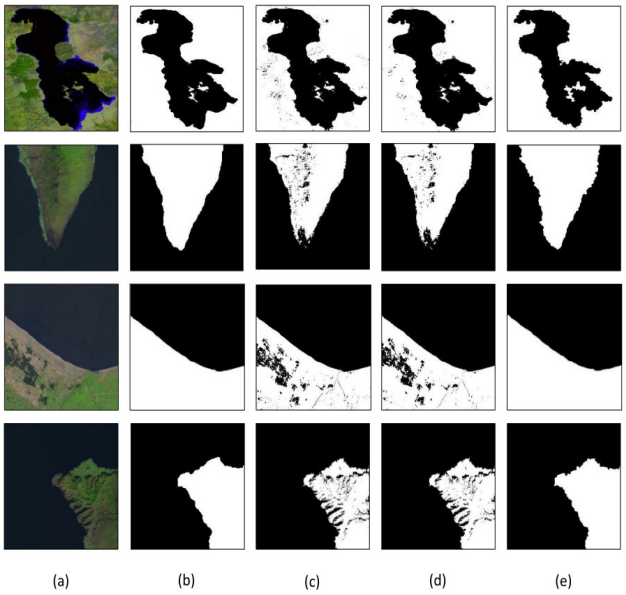

FIGURE 6. The results of the clustering methods. (a) original images, (b) Ground-truth, (c) FCM, (d) SFCM, and (e) SPFCM.

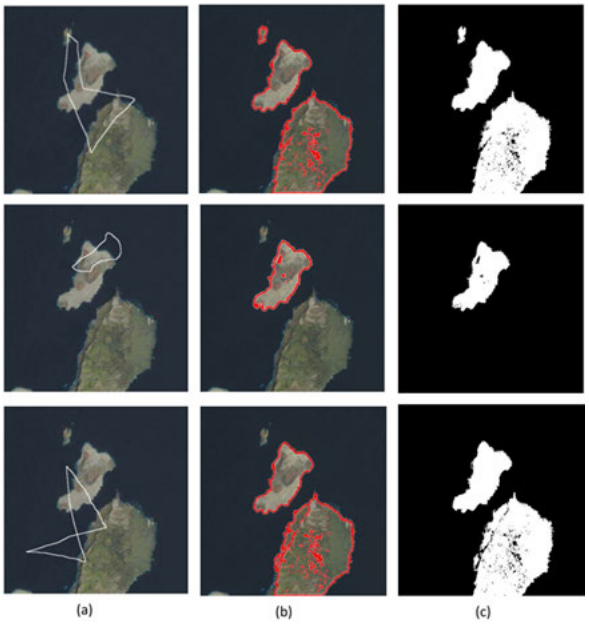

FIGURE 7. The results of the traditional CV model with different initial contours. (a) Original images with initial contour, (b) Final contours, and (c) The segmented images.

pixels in the land region due to mixed pixels and low contrast. These drawbacks produced unsatisfactory results. The SFCM clustering method incorporates pixel spatial information by adding an averaging neighborhood term added to the objective function to improve the accuracy and results. However, the local neighborhood size impacted the clustering process of the pixel. However, SFCM cannot achieve good results because it cannot capture all the complicated properties of images. As illustrated in Fig. 7, images are not smoothed and have some regions that appear dark as the sea. The proposed SPFCM achieves good results compared with FCM and SFCM clustering methods. SPFCM method clusters the image into regions based on superpixels, not the pixels as in the aforementioned methods. As illustrated in Fig. 7, SPFCM clusters the inhomogeneous images effectively. It has the ability to deal with rough images and the presence of pixel interference because SPFCM incorporates superpixel and its neighbors in the objective function. Also, it captures spectral, statistical, and texture features of the superpixel and its neighborhood to achieve efficient segmentation results.

TABLE 1. The performance of the fuzzy clustering methods.

Method	JSC (%)	DSC (%)	Recall (%)	Precision (%)	ACC (%)
FCM [39]	93.1	96.2	93.3	99.8	97.5
SFCM [68]	93.5	96.5	93.7	99.8	97.7
SPFCM	96.7	98.3	97.7	99	98.9

For quantitative analysis, JSC, DSC, ACC, Recall, and Precision are calculated and presented in Table 1. Regarding the performance comparison results. The higher performance is achieved using the SPFCM clustering rather than SFCM and FCM. The proposed SPFCM achieved an average accuracy of 98.9%, an average JSC of 96.7%, an average DSC of 98.3%, an average recall of 97.7%, and an average precision of 99%. As a result, SPFCM outperforms the SFCM and FCM clustering methods.

3) COMPARISON WITH POPULAR FUZZY-BASED ACMS

In this section, different fuzzy-based active contour models have been tested and compared with the proposed technique. Recently, many fuzzy-based ACMs have been proposed to enhance the robustness of the traditional CV model to low contrast and intensity inhomogeneity [14], [15], [19]. Fig. 8 shows the comparison of different fuzzy ACMs and the proposed technique. AS shown, the KFAC method misclassified some regions in the images with low contrast and intensity inhomogeneity. KFAC relies on the global information of the image in image segmentation.

On the other hand, the FRAGL model could not efficiently deal with the intensity inhomogeneity and low contrast of the image. The average of the FRAGL model depended on the incorporation of local and global intensities. This average may not fit the image's local information since the global average may differ from the actual image intensity. Finally, the GLFIF method segmented the images of low contrast and intensity inhomogeneity. However, these results were not accurate at the boundary. There are misclassifications in some sea regions, which were classified as land regions. The proposed method has achieved good segmentation results compared with fuzzy-based ACMs. The proposed method outperformed the mentioned fuzzy ACMs because it incorporates the textural, spectral, and spatial features,

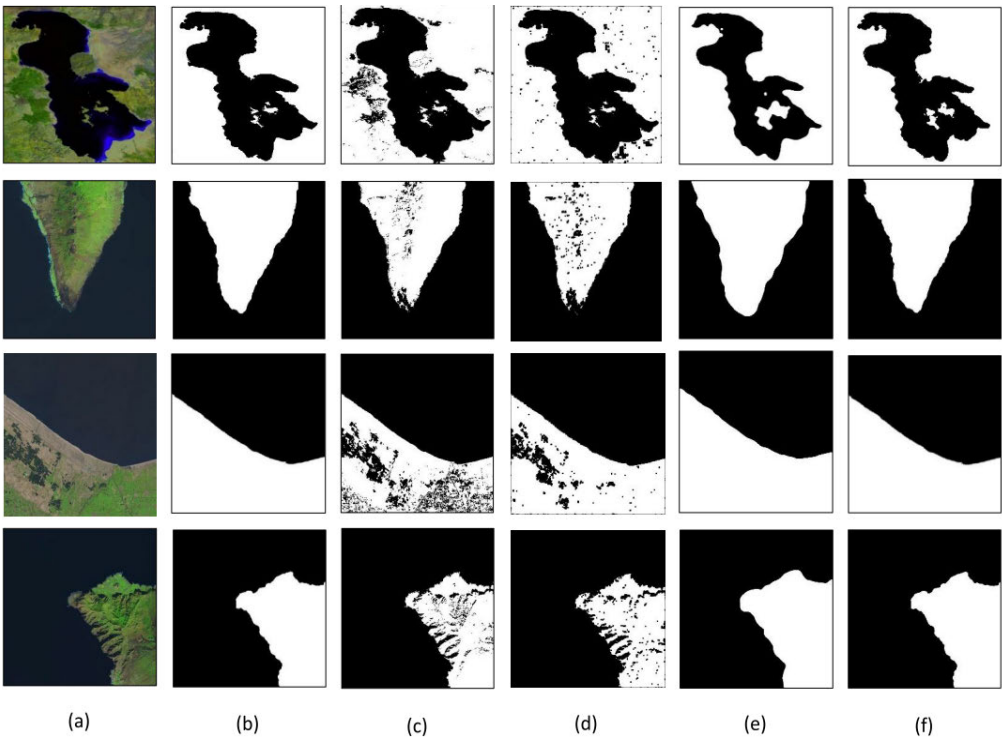

FIGURE 8. The results of fuzzy ACMs and the proposed method. (a) Original images, (b) Ground-truth, (c) KFAC, (d) FRAGL, (e) GLFIF, and (f) The proposed method.

TABLE 2. The performance of the fuzzy ACMs and the proposed method.

Method	JSC (%)	DSC (%)	Recall (%)	Precision (%)	ACC (%)
KFAC [14]	90.5	94.7	90.6	99.9	96.3
FRAGL [15]	94.1	96.8	94.3	99.7	96.9
GLFIF [19]	86.6	91.1	94	92.3	93.3
The Proposed	97.1	98.5	99.3	97.7	98.9

which enable the proposed method to deal with the image inhomogeneity.

For quantitative analysis, JSC, DSC, ACC, Recall, and Precision are calculated and presented in Table 2. Regarding the performance comparison results. The higher performance is achieved using the proposed method rather than KFAC, FRAGL, and GLFIF. The proposed method achieved an The average accuracy of 98.9%, an average JSC of 97.1%, an average DSC of 98.5%, an average recall of 99.3%, and an average precision of 97.7%. As a result, the proposed method outperforms the fuzzy ACMs.

4) COMPARISON WITH STATE-OF-THE-ART SLS METHODS

In this section, the efficiency of the proposed method is evaluated, and the results are compared with state-of-the-art methods, which are LBP [25], SMS [28], SFC [30], and traditional CV model [46], as shown in Fig. 9. As illustrated from the results, SMS, LBP, SFC, and CV methods produce segmentation results with misclassification in the land regions. This is because some images in the land regions are dark as the sea due to low illumination and low contrast between the sea and land. Besides, images have complex boundaries, complex texture, and intensity inhomogeneity of land area. The structural information, which LBP acquires, is limited. Only the pixel difference is used, and the magnitude information is ignored. The CV model is sensitive to initial contour, which can influence segmentation results. The CV with manual contour cannot deal with complex texture. SFC clusters images based on spatial information. However, it produces misclassification in results because it cannot deal with all the complicated properties of images and cannot capture texture information. The proposed method produces precise segmentation results that are consistent with correspondence ground-truth. As shown in Fig. 9, the proposed method segments the images with mixed pixels, intensity inhomogeneity, and rough texture.

For quantitative analysis, JSC, DSC, ACC, Recall, and Precision are calculated and presented in Table 3. It shows The performance of the state-of-the-art methods is compared with the proposed technique. The higher performance is achieved using the proposed method rather than other comparative methods regarding the comparison measurements. The proposed SPFCM- MCV achieves an average accuracy of 98.9%, an average JSC of 97.1%, an average DSC of 98.5%, an average recall of 99.3%, and an average precision of 97.7%. As a result, the proposed SPFCM-MCV outperforms state-of-the-art methods.

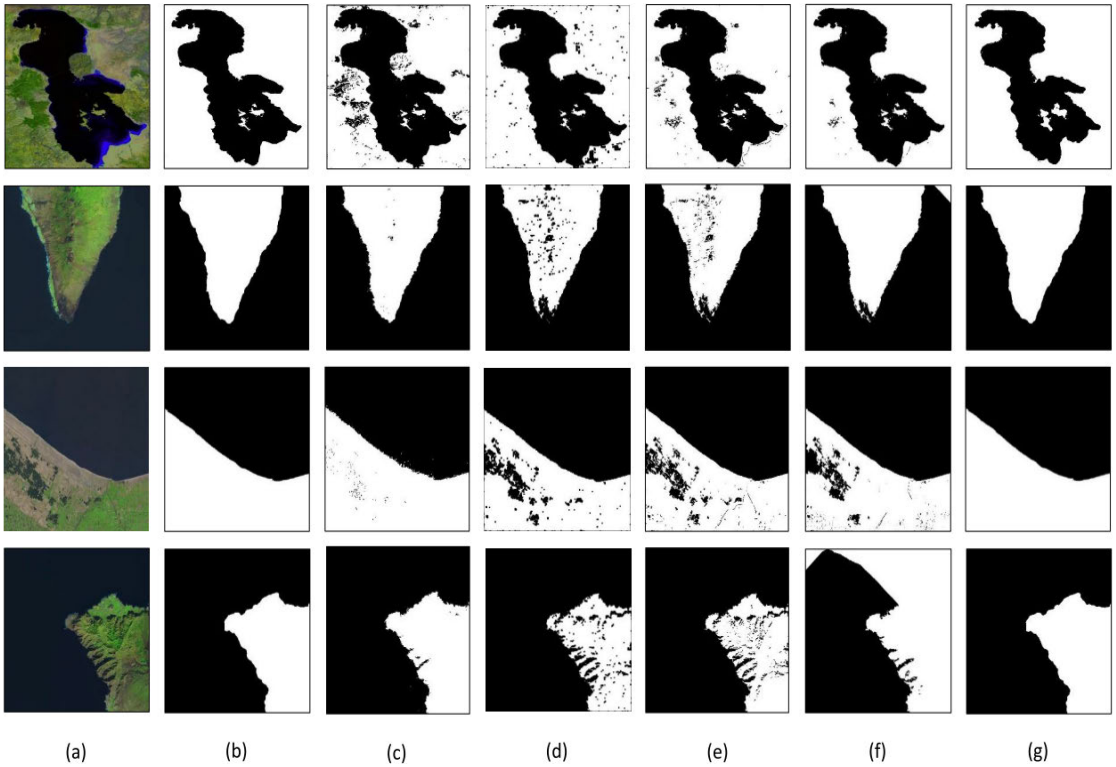

FIGURE 9. The results of different SLS methods. (a) Original images, (b) Ground-truth, (c) SMS, (d) LBP, (e) SFC, (f) Traditional CV, and (g) The Proposed Method.

TABLE 3. The comparison of the sls segmentation techniques.

Method	JSC (%)	DSC (%)	Recall (%)	Precision (%)	ACC (%)
SMS [28]	92.2	94.1	93.9	98.3	96.8
LBP [25]	89	94	89.1	99.9	95.7
SFC [30]	93.5	96.5	93.6	99.8	97.7
Traditional CV [46]	87	91.5	95.2	91.4	94.1
The Proposed	97.1	98.5	99.3	97.7	98.9

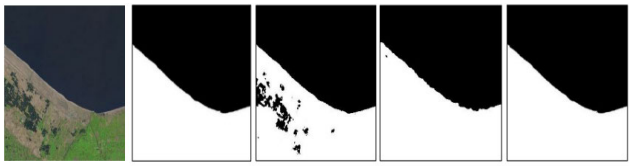

FIGURE 10. The trade-off between spatial and textural information. (a) Original images, (b) Ground-truth, (c) Spatial- based segmentation, (d) Textural- based segmentation, and (e) The Proposed Method.

5) THE TRADE-OFF BETWEEN SPATIAL AND TEXTURE INFORMATION

In this section, the trade-off between spatial and textural information is investigated. As shown in Fig. 10, the segmentation based only on the image's spatial information produces poor results. Also, textural information only is not sufficient to produce accurate results. As illustrated in the figure, the incorporation of spatial and textural information provides accurate segmentation of the image. As a result, the proposed method segments the image efficiently based on a combination of spatial and textural features.

6) DISCUSSION

The sea-land segmentation has a vital role in monitoring the changes in coastal zones, and water resources management, etc. Recently, Active contour models (ACMs) and Fuzzy clustering are powerful image segmentation methods due to their effective performance. FCM clustering approach can handle the fuzzy and uncertain data with mixed pixels. Besides, the CV active contour model considers image segmentation as an optimization problem. However, they can achieve poor results due to some challenges, such as an intensity inhomogeneity, low contrast between sea and land regions, and the large image size with redundant information.

Moreover, mixed pixels between sea and land regions and a complicated texture of the land cover area. All these challenges can impact the segmentation task for images. In addition, the CV model is sensitive to manual initialization. If the contour is incorrectly initialized, the CV model may produce incorrect results and take many iterations.

Motivated by the aforementioned observations, we proposed a novel unsupervised coarse-to-fine SLS technique for the natural colored RSIs. It integrates the SPFCM and the CV model for vector-valued images. The SPFCM clustering approach produces coarse sea-land

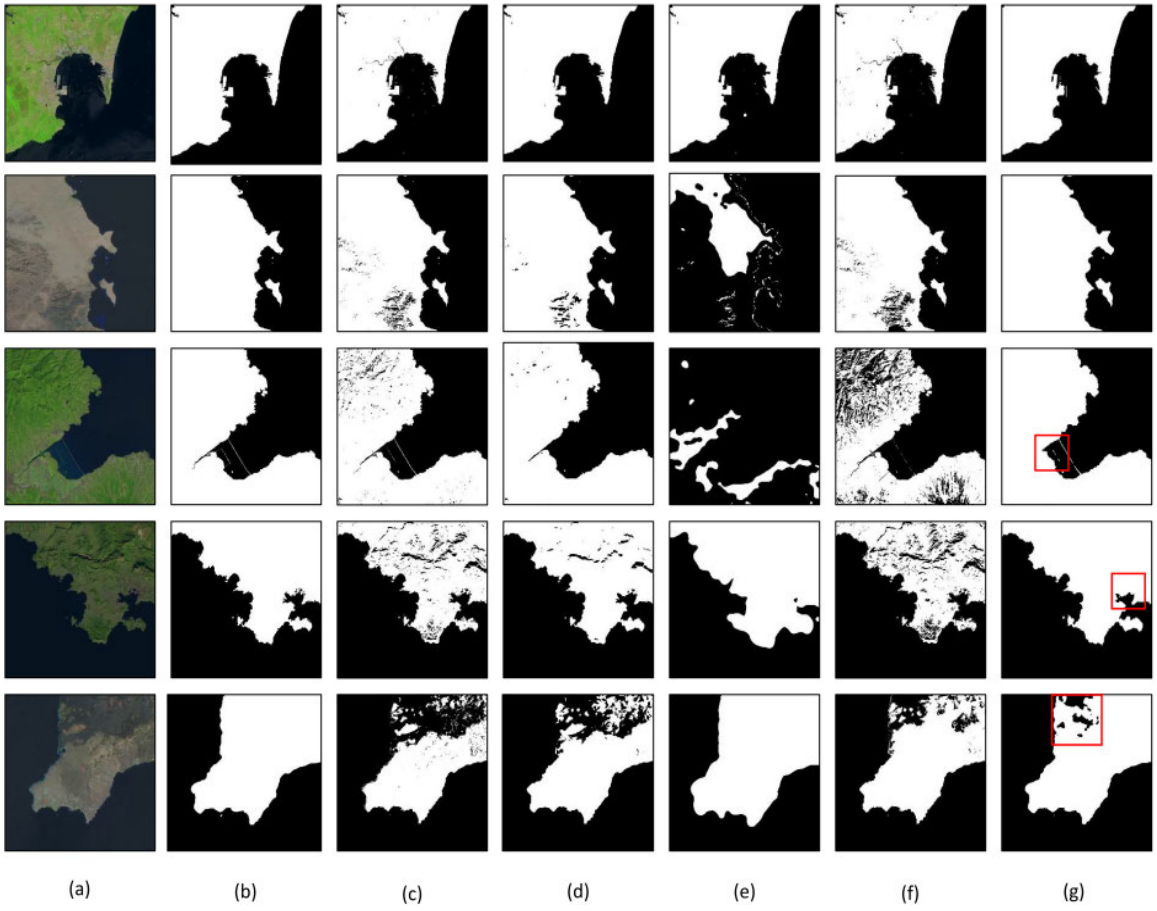

FIGURE 11. The segmentation results from different segmentation methods. (a) Original images, (b) Ground-truth, (c) KFAC, (d) FRAGL, (e) GLFIF, (f) Traditional CV, and (g) The Proposed Method.

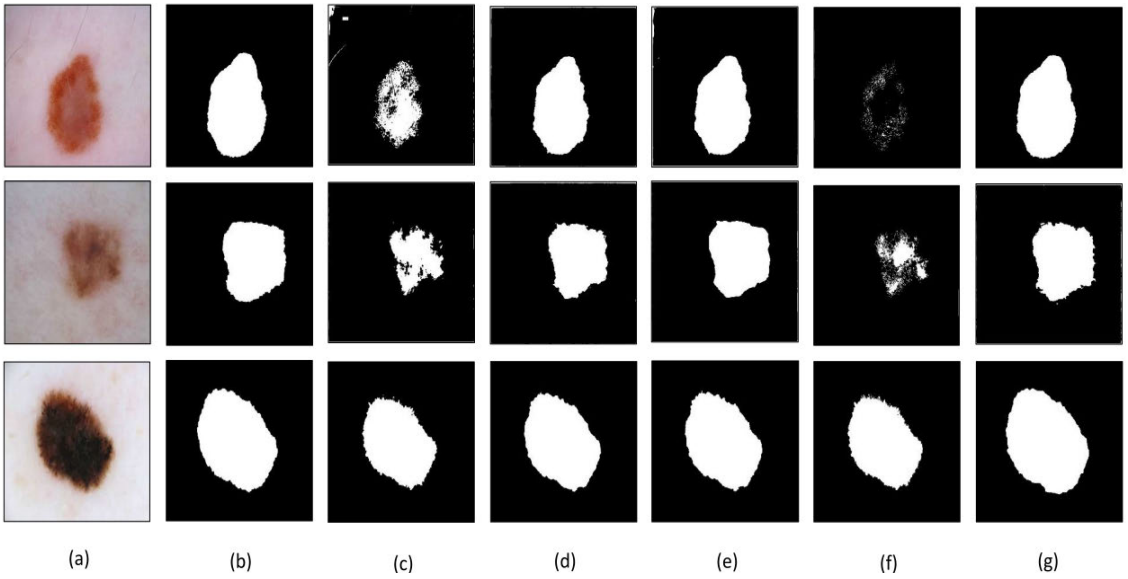

FIGURE 12. The segmentation results of skin lesion. (a) Original images, (b) Ground-truth, (c) KFAC, (d) FRAGL, (e) GLFIF, (f) Traditional CV, and (g) The Proposed Method.

segmentation results, which provides an automatic initial contour for the CV active contour model instead of manual initialization to improve the CV model's performance. Moreover, spectral color and texture features are combined to improve the CV model to solve its limitations to those complicated nature images with intensity inhomogeneity

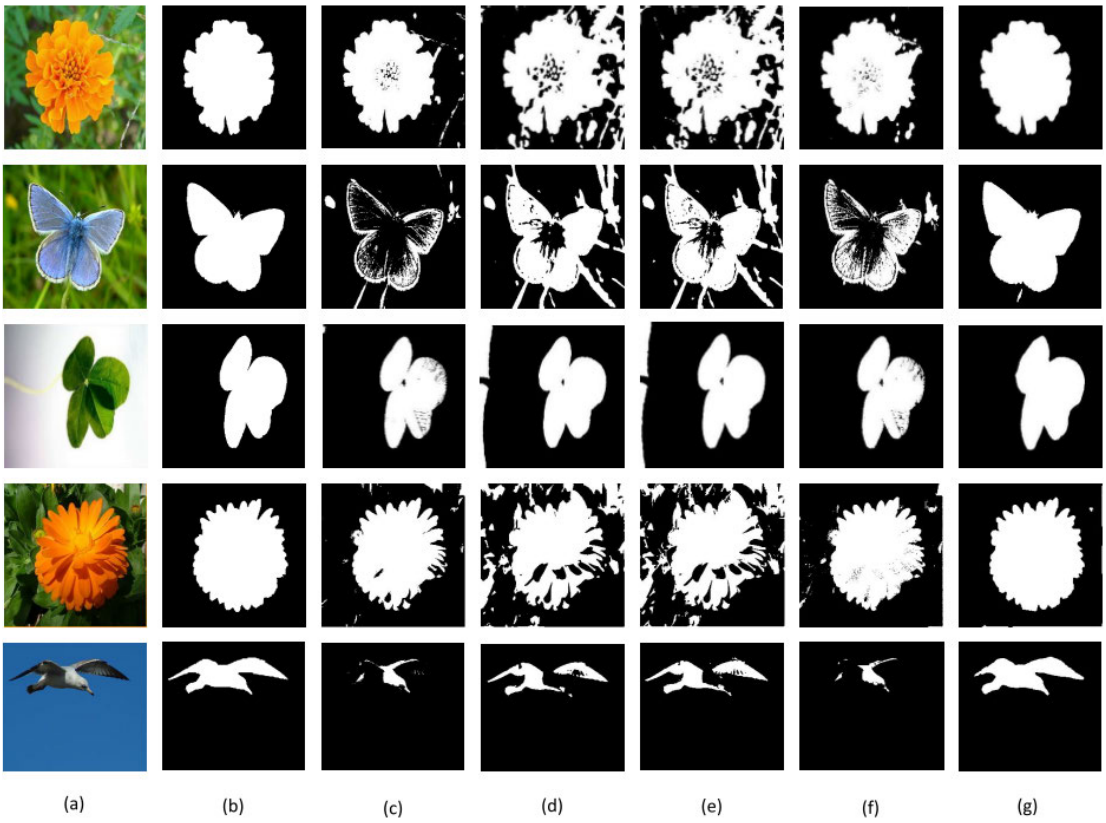

FIGURE 13. The segmentation results of natural images from MSRA-B and MSRA 10K. (a) Original images, (b) Ground-truth, (c) KFAC, (d) FRAGL, (e) GLFIF, (f) Traditional CV, and (g) The Proposed Method.

or rich texture features and produce fine segmentation results.

The proposed method's effectiveness is confirmed in fuzzy ACMs and SLS methods, as illustrated in the Results section. However, some over-segmentation and under-segmentation cases appear in our segmentation results compared with other recent segmentation methods, as shown in Fig. 11 in the Appendix. Also, Fig. 11 illustrated more case studies. The over-segmentation appeared when the sea's pixels were misclassified to a land region, as presented in the third and the fourth rows in Fig. 11. The over-segmentation problem appears in thin and extended regions of sea areas that are misclassified to land areas by the proposed method, as noticed in regions surrounded by red squares.

On the other hand, under-segmentation is misclassification of the land region where land's pixels are misclassified to a sea region. As shown in the fifth row in Fig. 11, this problem occurs only in the volcanic land regions. The proposed method cannot classify well the mixed volcanic and non-volcanic regions. It classifies these regions as a sea region. Regardless of that, the proposed method performs well, as presented in Fig. 8 and Fig. 9.

Moreover, the proposed strategy is tested on other application areas such as skin lesion segmentation and natural color images. The experimental results are shown in Fig.12 and Fig.13 in the Appendix. As presented in the results, the proposed method works well in other applications and outperforms state-of-the-art methods, which poorly achieve segmentation results.

The following are some of the possible future directions in sea-land image segmentation. The first one may apply feature fusion from multiscale analysis, such as wavelet analysis, to improve the performance. Also, integrating SPFCM with graph-cut image segmentation is excepted to produce better results. Moreover, an optimization tool such as particle swarm optimization (PSO) or genetic algorithm may be used to produce an optimal initial contour for ACMs.

VI. CONCLUSION

In this paper, a modified CV active contour method and SPFCM method are incorporated to segment sea-land remote sensing images into sea and land regions. RSIs have a large size with redundant data and often low contrast. The proposed the method overcomes the presented limitations either in optical remote sensing images or traditional segmentation methods. The traditional SLS methods produced inaccurate results because they ignore spatial context and cannot overcome the image's complicated characteristics. This paper utilizes the image's spectral and spatial information by over-segmenting superpixels' images to reduce information redundancy and utilize spectral and spatial information. The SPFCM clustering approach employs the local relationship

among neighboring superpixels. This is done to cluster superpixels based on the color and texture features to produce coarse SLS results, which are utilized as an initial contour for the modified CV model instead of manual initialization. This initial contour reduces the number of iterations and computational time of the CV model. Finally, the color and texture features are incorporated to improve the CV. It solves the CV model's problems and produces unsatisfactory results for naturally complicated images with intensity inhomogeneity or complex texture. The experiment results demonstrated that the proposed method effectively segments the image and achieves high accuracy compared with state-of-the-art methods. In the future, feature fusion from multiscale analysis, such as wavelet analysis, will improve the performance. Moreover, an optimization tool such as particle swarm optimization (PSO) or genetic algorithm may be used to produce an optimal initial contour for ACMs. Also, integrating SPFCM with graph-cut image segmentation is excepted to produce better results.

APPENDIX

This section presents extra the experimental results of more case studies and other applications area from the proposed method compared with other segmentation methods.

AUTHOR CONTRIBUTIONS

Conceptualization, E.E., H.S., A.A., N.M. and M.E.; methodology, E.E., H.S., A.A., N.M. and M.E.; software, E.E., N.M., and H.S.; validation, M.E. and K.K; formal analysis, E.E., N.M., and H.S.; investigation, K.K., and M.E.; resources, H.S. and K.K.; data curation, E.E., and M.E.; writing—original draft preparation, E.E., H.S., A.A., N.M., and M.E.; writing—review and editing, H.S., N.M., K.K., and M.E.; visualization, E.E., K.K., and M.E.; supervision, N.M. and H.S.; project administration, H.S., and N.M.; funding acquisition, K.K. All authors have read and agreed to the published version of the manuscript.

CONFLICTS OF INTEREST

The authors declare no conflict of interest.

REFERENCES

[1] V. Paravolidakis, L. Ragia, K. Moirogiorgou, and M. Zervakis, "Automatic coastline extraction using edge detection and optimization procedures," *Geosciences*, vol. 8, no. 11, p. 407, Nov. 2018, doi: 10.3390/geosciences8110407.

[2] R. Aedla, G. S. Dwarakish, and D. V. Reddy, "Automatic shoreline detection and change detection analysis of Netravati-GurpurRivermouth using histogram equalization and adaptive thresholding techniques," *Aquatic Procedia*, vol. 4, pp. 563–570, Jan. 2015, doi: 10.1016/j.aqpro.2015.02.073.

[3] G. Liu, Y. Zhang, X. Zheng, X. Sun, K. Fu, and H. Wang, "A new method on inshore ship detection in high-resolution satellite images using shape and context information," *IEEE Geosci. Remote Sens. Lett.*, vol. 11, no. 3, pp. 617–621, Mar. 2014, doi: 10.1109/lgrs.2013.2272492.

[4] D. Cheng, G. Meng, S. Xiang, and C. Pan, "FusionNet: Edge aware deep convolutional networks for semantic segmentation of remote sensing harbor images," *IEEE J. Sel. Topics Appl. Earth Observ. Remote Sens.*, vol. 10, no. 12, pp. 5769–5783, Dec. 2017, doi: 10.1109/jstars.2017.2747599.

[5] U. R. Aktas, G. Can, and F. T. Y. Vural, "Edge-aware segmentation in satellite imagery: A case study of shoreline detection," in *Proc. 7th IAPR Workshop Pattern Recognit. Remote Sens. (PRRS)*, Nov. 2012, pp. 1–4, doi: 10.1109/pprs.2012.6398319.

[6] N. Wang, B. Li, Q. Xu, and Y. Wang, "Automatic ship detection in optical remote sensing images based on anomaly detection and SPP-PCANet," *Remote Sens.*, vol. 11, no. 1, p. 47, Dec. 2018, doi: 10.3390/rs11010047.

[7] D. Cheng, G. Meng, S. Xiang, and C. Pan, "Efficient sea–land segmentation using seeds learning and edge directed graph cut," *Neurocomputing*, vol. 207, pp. 36–47, Sep. 2016, doi: 10.1016/j.neucom.2016.04.020.

[8] J. P. Ferreira and J. M. Bioucas-Dias, "Bayesian land and sea segmentation of SAR imagery," in *Proc. TerraSAR-X Sci. Team Meeting*, Oberpfaffenhofen, Germany, 2008. [Online]. Available: http://sss.terrasar-x.dlr.de/papers_sci_meet_3/paper/.OCE0050_ferreira.pdf

[9] C. Mao and S. Wan, "A water/land segmentation algorithm based on an improved Chan-Vese model with edge constraints of complex wavelet domain," *Chin. J. Electron.*, vol. 24, no. 2, pp. 361–365, Apr. 2015, doi: 10.1049/cje.2015.04.023.

[10] K. Saini and S. Arora, "A study analysis on the different image segmentation techniques," *Int. J. Inf. Comput. Technol., Int. Res. Publications House*, vol. 4, no. 14, pp. 1445–1452, 2014.

[11] D. Kaur and Y. Kaur, "Various image segmentation techniques: A review," *Int. J. Comput. Sci. Mobile Comput.*, vol. 3, no. 5, pp. 809–814, 2014.

[12] S. Lei, Z. Zou, D. Liu, Z. Xia, and Z. Shi, "Sea-land segmentation for infrared remote sensing images based on superpixels and multi-scale features," *Infr. Phys. Technol.*, vol. 91, pp. 12–17, Jun. 2018, doi: 10.1016/j.infrared.2018.03.012.

[13] L. Ma, N. Q. Soomro, J. Shen, L. Chen, Z. Mai, and G. Wang, "Hierarchical sea-land segmentation for panchromatic remote sensing imagery," *Math. Problems Eng.*, vol. 2017, pp. 1–8, Mar. 2017, doi: 10.1155/2017/4728425.

[14] Y. Wu, W. Ma, M. Gong, H. Li, and L. Jiao, "Novel fuzzy active contour model with kernel metric for image segmentation," *Appl. Soft Comput.*, vol. 34, pp. 301–311, Sep. 2015, doi: 10.1016/j.asoc.2015.04.058.

[15] J. Fang, H. Liu, L. Zhang, J. Liu, and H. Liu, "Fuzzy region-based active contours driven by weighting global and local fitting energy," *IEEE Access*, vol. 7, pp. 184518–184536, 2019, doi: 10.1109/access.2019.2909981.

[16] W. Zhao, X. Xu, Y. Zhu, and F. Xu, "Active contour model based on local and global Gaussian fitting energy for medical image segmentation," *Optik*, vol. 158, pp. 1160–1169, Apr. 2018, doi: 10.1016/j.ijleo.2018.01.004.

[17] R. Jin and G. Weng, "A robust active contour model driven by fuzzy C-means energy for fast image segmentation," *Digit. Signal Process.*, vol. 90, pp. 100–109, Jul. 2019, doi: 10.1016/j.dsp.2019.04.004.

[18] S. Soomro, A. Munir, and K. N. Choi, "Fuzzy C-means clustering based active contour model driven by edge scaled region information," *Expert Syst. Appl.*, vol. 120, pp. 387–396, Apr. 2019, doi: 10.1016/j.eswa.2018.10.052.

[19] J. Fang, H. Liu, J. Liu, H. Zhou, L. Zhang, and H. Liu, "Fuzzy region-based active contour driven by global and local fitting energy for image segmentation," *Appl. Soft Comput.*, vol. 100, Mar. 2021, Art. no. 106982, doi: 10.1016/j.asoc.2020.106982.

[20] W. Liu, L. Ma, H. Chen, Z. Han, and N. Q. Soomro, "Sea–land segmentation for panchromatic remote sensing imagery via integrating improved MNcut and Chan–Vese model," *IEEE Geosci. Remote Sens. Lett.*, vol. 14, no. 12, pp. 2443–2447, Dec. 2017, doi: 10.1109/lgrs.2017.2768300.

[21] R. Li, W. Liu, L. Yang, S. Sun, W. Hu, F. Zhang, and W. Li, "DeepUNet: A deep fully convolutional network for pixel-level sea-land segmentation," *IEEE J. Sel. Topics Appl. Earth Observ. Remote Sens.*, vol. 11, no. 11, pp. 3954–3962, Nov. 2018, doi: 10.1109/jstars.2018.2833382.

[22] T. Lei, X. Jia, Y. Zhang, S. Liu, H. Meng, and A. K. Nandi, "Superpixel-based fast fuzzy C-means clustering for color image segmentation," *IEEE Trans. Fuzzy Syst.*, vol. 27, no. 9, pp. 1753–1766, Sep. 2019, doi: 10.1109/tfuzz.2018.2889018.

[23] S. N. Kumar, A. L. Fred, and P. S. Varghese, "Suspicious lesion segmentation on brain, mammograms and breast MR images using new optimized spatial feature based super-pixel fuzzy C-means clustering," *J. Digit. Imag.*, vol. 32, no. 2, pp. 322–335, Apr. 2019, doi: 10.1007/s10278-018-0149-9.

[24] C. Li, L. Liu, X. Sun, J. Zhao, and J. Yin, "Image segmentation based on fuzzy clustering with cellular automata and features weighting," *EURASIP J. Image Video Process.*, vol. 2019, no. 1, pp. 1–11, Dec. 2019, doi: 10.1186/s13640-019-0436-5.

[25] Y. Xia, S. Wan, P. Jin, and L. Yue, "A novel sea-land segmentation algorithm based on local binary patterns for ship detection," *Int. J. Signal Process., Image Process. Pattern Recognit.*, vol. 7, no. 3, pp. 237–246, Jun. 2014, doi: 10.14257/ijsip.2014.7.3.19.

[26] Y. Zhuang, D. Guo, H. Chen, F. Bi, L. Ma, and N. Q. Soomro, "A novel sea-land segmentation based on integral image reconstruction in MWIR images," *Sci. China Inf. Sci.*, vol. 60, no. 6, Jun. 2017, doi: 10.1007/s11432-016-0410-3.

[27] D. Vukadinov, R. Jovanovic, and M. Tuba, "An algorithm for coastline extraction from satellite imagery," *Int. J. Comput.*, vol. 2, pp. 8–15, 2017.

[28] X. You and W. Li, "A sea-land segmentation scheme based on statistical model of sea," in *Proc. 4th Int. Congr. Image Signal Process.*, Oct. 2011, pp. 1155–1159, doi: 10.1109/cisp.2011.6100503.

[29] P. Wang, Y. Zhuang, H. Chen, L. Chen, H. Shi, and F. Bi, "Pyramid integral image reconstruction algorithm for infrared remote sensing sea-land segmentation," in *Proc. IEEE Int. Geosci. Remote Sens. Symp. (IGARSS)*, Jul. 2017, pp. 3763–3766, doi: 10.1109/igarss.2017.8127818.

[30] M. Modava and G. Akbarizadeh, "Coastline extraction from SAR images using spatial fuzzy clustering and the active contour method," *Int. J. Remote Sens.*, vol. 38, no. 2, pp. 355–370, Jan. 2017, doi: 10.1080/01431161.2016.1266104.

[31] P. Rachee, "Segmentation of satellite imagery of Amedi site using Chan–Vese model with saliency estimation," *J. Appl. Sci. Technol. Trends*, vol. 1, no. 4, pp. 125–134, Dec. 2020, doi: 10.38094/jastt1454.

[32] V. Rajinikanth, N. Dey, R. Kumar, J. Panneerselvam, and N. S. M. Raja, "Fetal head periphery extraction from ultrasound image using Jaya algorithm and Chan–Vese segmentation," *Procedia Comput. Sci.*, vol. 152, pp. 66–73, Jan. 2019, doi: 10.1016/j.procs.2019.05.028.

[33] R. Achanta, A. Shaji, K. Smith, A. Lucchi, P. Fua, and S. Süsstrunk, "SLIC superpixels compared to state-of-the-art superpixel methods," *IEEE Trans. Pattern Anal. Mach. Intell.*, vol. 34, no. 11, pp. 2274–2282, Nov. 2012, doi: 10.1109/tpami.2012.120.

[34] H. Li, Y. Shi, B. Zhang, and Y. Wang, "Superpixel-based feature for aerial image scene recognition," *Sensors*, vol. 18, no. 2, p. 156, Jan. 2018, doi: 10.3390/s18010156.

[35] R. Kusumaningrum and A. M. Arymurthy, "Color and texture feature for remote sensing-image retrieval system: A comparative study," *Int. J. Comput. Sci. Issues*, vol. 8, no. 5, p. 125, 2011.

[36] M. H. Shakoor and F. Tajeripour, "Noise robust and rotation invariant entropy features for texture classification," *Multimedia Tools Appl.*, vol. 76, no. 6, pp. 8031–8066, Mar. 2017, doi: 10.1007/s11042-016-3455-6.

[37] J. Kapur, P. Sahoo, and A. Wong, "A new method for gray-level picture thresholding using the entropy of the histogram," *Comput. Vis., Graph., Image Process.*, vol. 29, no. 1, p. 140, 1985, doi: 10.1016/s0734-189x(85)90156-2.

[38] X. Kang, G. Gao, Q. Hao, and S. Li, "A Coarse-to-Fine method for cloud detection in remote sensing images," *IEEE Geosci. Remote Sens. Lett.*, vol. 16, no. 1, pp. 110–114, Jan. 2019, doi: 10.1109/lgrs.2018.2866499.

[39] J. C. Dunn, "A fuzzy relative of the ISODATA process and its use in detecting compact well-separated clusters," *J. Cybern.*, vol. 3, no. 3, pp. 32–57, Jan. 1973, doi: 10.1080/01969727308546046.

[40] J. C. Bezdek, "A convergence theorem for the fuzzy ISODATA clustering algorithms," *IEEE Trans. Pattern Anal. Mach. Intell.*, vol. PAMI-2, no. 1, pp. 1–8, Jan. 1980, doi: 10.1109/tpami.1980.4766964.

[41] G. Dougherty, "Unsupervised learning," in *Pattern Recognition and Classification*. Sep. 2012, pp. 143–155, doi: 10.1007/978-1-4614-5323-9_8.

[42] A. Srinivasan and S. Sadagopan, "Rough fuzzy region based bounded support fuzzy C-means clustering for brain MR image segmentation," *J. Ambient Intell. Humanized Comput.*, pp. 1–14, Jan. 2020, doi: 10.1007/s12652-019-01672-w.

[43] X. Yang and X. Jiang, "A hybrid active contour model based on new edge-stop functions for image segmentation," *Int. J. Ambient Comput. Intell.*, vol. 11, no. 1, pp. 87–98, Jan. 2020, doi: 10.4018/IJACI.2020010105.

[44] S. Jia and C. Zhang, "Fast and robust image segmentation using an superpixel based FCM algorithm," in *Proc. IEEE Int. Conf. Image Process. (ICIP)*, Oct. 2014, pp. 947–951, doi: 10.1109/icip.2014.7025190.

[45] S. K. Adhikari, J. K. Sing, D. K. Basu, and M. Nasipuri, "Conditional spatial fuzzy C-means clustering algorithm for segmentation of MRI images," *Appl. Soft Comput.*, vol. 34, pp. 758–769, Sep. 2015, doi: 10.1016/j.asoc.2015.05.038.

[46] T. F. Chan and L. A. Vese, "Active contours without edges," *IEEE Trans. Image Process.*, vol. 10, no. 2, pp. 266–277, 2001, doi: 10.1109/83.902291.

[47] B. Han, Y. Wu, and Y. Song, "A novel active contour model based on median absolute deviation for remote sensing river image segmentation," *Comput. Electr. Eng.*, vol. 62, pp. 209–223, Aug. 2017, doi: 10.1016/j.compeleceng.2017.04.005.

[48] Y. Song, Y. Wu, and Y. Dai, "A new active contour remote sensing river image segmentation algorithm inspired from the cross entropy," *Digit. Signal Process.*, vol. 48, pp. 322–332, Jan. 2016, doi: 10.1016/j.dsp.2015.10.005.

[49] T. F. Chan, B. Y. Sandberg, and L. A. Vese, "Active contours without edges for vector-valued images," *J. Vis. Commun. Image Represent.*, vol. 11, no. 2, pp. 130–141, Jun. 2000, doi: 10.1006/jvci.1999.0442.

[50] L. A. Vese and T. F. Chan, "A multiphase level set framework for image segmentation using the Mumford and shah model," *Int. J. Comput. Vis.*, vol. 50, no. 3, pp. 271–293, 2002, doi: 10.1023/a:1020874308076.

[51] H. Min, W. Jia, X.-F. Wang, Y. Zhao, R.-X. Hu, Y.-T. Luo, F. Xue, and J.-T. Lu, "An intensity-texture model based level set method for image segmentation," *Pattern Recognit.*, vol. 48, no. 4, pp. 1547–1562, Apr. 2015, doi: 10.1016/j.patcog.2014.10.018.

[52] X. Huang, H. Bai, and S. Li, "Automatic aerial image segmentation using a modified Chan–Vese algorithm," in *Proc. 9th IEEE Conf. Ind. Electron. Appl.*, Jun. 2014, pp. 1091–1094, doi: 10.1109/iciea.2014.6931327.

[53] S. Toure, O. Diop, K. Kpalma, and A. S. Maiga, "Best-performing color space for land-sea segmentation," in *Proc. 41st Int. Conf. Telecommun. Signal Process. (TSP)*, Jul. 2018, pp. 1–5, doi: 10.1109/tsp.2018.8441437.

[54] S. Toure, O. Diop, K. Kpalma, and A. S. Maiga, "Coastline detection using fusion of over segmentation and distance regularization level set evolution," *ISPRS-Int. Arch. Photogramm., Remote Sens. Spatial Inf. Sci.*, vol. XLII-3/W4, pp. 513–518, Mar. 2018, doi: 10.5194/isprs-archives-xlii-3-w4-513-2018.

[55] Z. Gharibbafghi, J. Tian, and P. Reinartz, "Modified superpixel segmentation for digital surface model refinement and building extraction from satellite stereo imagery," *Remote Sens.*, vol. 10, no. 11, p. 1824, Nov. 2018, doi: 10.3390/rs10111824.

[56] D. Cheng, G. Meng, G. Cheng, and C. Pan, "SeNet: Structured edge network for sea-land segmentation," *IEEE Geosci. Remote Sens. Lett.*, vol. 14, no. 2, pp. 247–251, Feb. 2017, doi: 10.1109/lgrs.2016.2637439.

[57] Y. Wicaksono, R. Wahono, and V. Suhartono, "Color and texture extraction using Gabor filter-local binary pattern for image segmentation with fuzzy C-means," *J. Intell. Syst.*, vol. 1, no. 1, pp. 15–21, 2015.

[58] M. H. Bharati, J. J. Liu, and J. F. MacGregor, "Image texture analysis: Methods and comparisons," *Chemometric Intell. Lab. Syst.*, vol. 72, no. 1, pp. 57–71, Jun. 2004, doi: 10.1016/j.chemolab.2004.02.005.

[59] M. Tsaneva, "Texture features for segmentation of satellite images," *Cybern. Inf. Technol.*, vol. 8, no. 3, pp. 73–85, 2008.

[60] L. Davis, "Image texture analysis techniques—A survey," in *Digital Image Processing*. Cham, Switzerland: Springer, 1981, pp. 189–201, doi: 10.1007/978-94-009-8543-8_11.

[61] P. Devalatkar and P. Patavardhan, "Image texture analysis—A survey," in *Proc. Int. Conf. Adv. Comput. Manage. (ICACM)*, Jaipur, India, Apr. 2019, pp. 1–5, doi: 10.2139/ssrn.3446546.

[62] H. Lv, S. Fu, C. Zhang, and X. Liu, "Non-local weighted fuzzy energy-based active contour model with level set evolution starting with a constant function," *IET Image Process.*, vol. 13, no. 7, pp. 1115–1123, May 2019, doi: 10.1049/iet-ipr.2018.5420.

[63] E. A. Zanaty, S. Aljahdali, and N. Debnath, "A kernelized fuzzy c-means algorithm for automatic magnetic resonance image segmentation," *J. Comput. Methods Sci. Eng.*, vol. 9, no. s2, pp. S123–S136, Jul. 2009, doi: 10.3233/jcm-2009-0241.

[64] P. Ahmadi, S. Sadri, R. Amirfattahi, and N. Gheissari, "Automatic aerial image segmentation based on a modified Chan-Vese algorithm," in *Proc. 5th Int. Congr. Image Signal Process.*, Oct. 2012, pp. 643–647, doi: 10.1109/cisp.2012.6469766.

[65] Glovis.usgs.gov. (2020)*GloVis-Home*. Accessed: Dec. 29, 2020. [Online]. Available: https://glovis.usgs.gov/

[66] H. Ali, M. Elmogy, E. ALdaidamony, and A. Atwan, "MRI brain image segmentation based on cascaded fractional-order darwinian particle swarm optimization and mean shift," *Int. J. Intell. Comput. Inf. Sci.*, vol. 15, no. 1, pp. 71–83, Jan. 2015, doi: 10.21608/ijicis.2015.10912.

[67] M. R. Ibraheem, S. El-Sappagh, T. Abuhmed, and M. Elmogy, "Staging melanocytic skin neoplasms using high-level pixel-based features," *Electronics*, vol. 9, no. 9, p. 1443, Sep. 2020, doi: 10.3390/electronics9091443.

[68] K.-S. Chuang, H.-L. Tzeng, S. Chen, J. Wu, and T.-J. Chen, "Fuzzy C-means clustering with spatial information for image segmentation," *Computerized Med. Imag. Graph.*, vol. 30, no. 1, pp. 9–15, Jan. 2006, doi: 10.1016/j.compmedimag.2005.10.001.
[69] A. S. Ashour, R. M. Nagieb, H. A. El-Khobby, M. M. A. Elnaby, and N. Dey, "Genetic algorithm-based initial contour optimization for skin lesion border detection," *Multimedia Tools Appl.*, vol. 80, no. 2, pp. 2583–2597, Jan. 2021, doi: 10.1007/s11042-020-09792-8.
[70] H. Jiang, J. Wang, Z. Yuan, Y. Wu, N. Zheng, and S. Li, "Salient object detection: A discriminative regional feature integration approach," in *Proc. IEEE Conf. Comput. Vis. Pattern Recognit.*, Jun. 2013, pp. 2083–2090, doi: 10.1109/CVPR.2013.271.
[71] M.-M. Cheng, N. J. Mitra, X. Huang, P. H. S. Torr, and S.-M. Hu, "Global contrast based salient region detection," *IEEE Trans. Pattern Anal. Mach. Intell.*, vol. 37, no. 3, pp. 569–582, Mar. 2015, doi: 10.1109/TPAMI.2014.2345401.

EMAN ELKHATEEB received the B.Sc. degree in information technology from the Faculty of Computers and Information, Mansoura University, Egypt, in 2012. She has been working as a Demonstrator with the Faculty of Computers and Information since 2012 until now. Her current research interests include remote sensing image analysis, image processing, and pattern recognition. She received Dr. Rushdi Amer Award for the Best Project on the 11th Egyptian Engineering Day in the field of computer programming from the Association of Electrical and Electronics Engineers–Egypt Branch, in September 2012.

HASSAN SOLIMAN received the B.Sc., M.Sc., and Ph.D. degrees in electronic communications engineering from the Faculty of Engineering, Mansoura University, Mansoura, Egypt, in 1983, 1987, and 1993, respectively. He worked as an Assistant Professor, an Associate Professor, and a Professor with the Faculty of Engineering, Mansoura University, from 1993 to 2016. From 1999 to 2002, he worked as a Visiting Associate Professor with the Department of Computer and Information, College of Telecom and Information, Riyadh, Saudi Arabia. From 2004 to 2009, he worked as a Visiting Associate Professor with the Department of Computer and Information, Taibah University, Medina, Saudi Arabia. He is currently a Professor of Information Technology and since 2015, he has been working as a Dean of the Faculty of Computers and Information, Mansoura University. He has authored/coauthored over 50 research publications in peer-reviewed reputed journals, book chapters, and conference proceedings. He advised more than 20 master's and doctoral graduates. His current research interests include computer networking, computer security, medical image analysis, and machine learning.

AHMED ATWAN received the B.Sc., M.Sc., and Ph.D. degrees in electronics and communications engineering from the Faculty of Engineering, Mansoura University, Egypt, in 1988, 1998, and 2004, respectively. From 2000 to 2004, he worked as a Lecturer with the Faculty of Technology, Al-Baha, Saudi Arabia. From 2005 to 2009, he worked as an Assistant Professor with the Faculty of Computers and Information Sciences (FCIS), Mansoura University. From 2010 to 2015, he worked as an Associate Professor with FCIS, Mansoura University. Since 2016, he has been working as a Professor with FCIS, Mansoura University. Since 2019 until now, he has also been working as a Professor with the Faculty of Computer and Information Technology, Northern Boarder University, Saudi Arabia. His research interests include pattern recognition, networking, signal processing, and image processing.

MOHAMMED ELMOGY (Senior Member, IEEE) received the B.Sc. and M.Sc. degrees from the Faculty of Engineering, Mansoura University, Mansoura, Egypt, and the Ph.D. degree from the Informatics Department, MIN Faculty, Hamburg University, Hamburg, Germany, in 2010. From July 2016 to August 2019, he worked as a Visiting Researcher with the Department of Bioengineering, University of Louisville, Louisville, KY, USA. He is currently an Associate Professor with the Information Technology Department, Faculty of Computers and Information, Mansoura University. He advised more than 30 master's and doctoral graduates. He has authored/coauthored over 200 research publications in peer-reviewed reputed journals, book chapters, and conference proceedings. His current research interests include computer vision, medical image analysis, machine learning, pattern recognition, and biomedical engineering. He is also a Professional Member of the ACM Society. He has served as a technical program committee member for many workshops and conferences. He has also served as a reviewer for various international journals.

KYUNG-SUP KWAK (Life Senior Member, IEEE) received the B.S. degree from Inha University, Inchon, South Korea, in 1977, the M.S. degree from the University of Southern California, in 1981, and the Ph.D. degree from the University of California at San Diego, in 1988, under the Inha University Fellowship and the Korea Electric Association Abroad Scholarship Grants, respectively. He worked with Hughes Network System, San Diego, CA, USA, and the IBM Network Research Center, USA, from 1988 to 1990. He has been with Inha University since 1990 as the Inha Fellow Professor, where he is currently the Inha Hanlim Professor and the Director of the UWB Wireless Communications Research Center, South Korea. His research interests include multiple access communication systems, mobile communication systems, UWB radio systems and ad-hoc networks, and the high performance wireless Internet. He is also a member of IEICE, KICS, and KIEE.

NAGHAM MEKKY received the B.Sc., M.Sc., and Ph.D. degrees in electronics communication engineering from Mansoura University, Mansoura, Egypt. She was a Researcher Assistant with the Department of Electronics Communication Engineering, Mansoura University, for seven years, before joining the Misr Higher Institute for Engineering and Technology, Mansoura, in 2007, as an Assistant Lecturer. She is currently an Assistant Professor with the Department of Information Technology, Faculty of Computers and Information Systems, Mansoura University. Her research interests include image processing, semantic web, the IoT, and biomedical engineering.